Coagulation-flocculation followed by catalytic ozonation processes for enhanced primary treatment during wet weather conditions

Núria López-Vinent[1], Alberto Cruz-Alcalde[1], Soliu O. Ganiyu[2], Shailesh Sable[2], Selamawit Ashagre Messele[2], Dustin Lillico[3], James Stafford[3], Carme Sans[1], Jaime Giménez[1], Santiago Esplugas[1*], Mohamed Gamal El-Din[2*]

[1]*Department of Chemical Engineering and Analytical Chemistry, Faculty of Chemistry, University of Barcelona, C/Martí i Franqués 1, 08028- Barcelona, Spain. Tel: +34934020154. Fax: +34934021291*

[2]*Department of Civil and Environmental Engineering, Faculty of Engineering North Campus, University of Alberta, 9211-116 Street NW, T6G 1H9 -Edmonton, Canada. Tel: 1-780-492-5124*

[3]*Department of Biological Sciences, 11355 - Saskatchewan Drive, University of Alberta, Edmonton, Alberta T6G 2E9, Canada. Tel: 1-780-492-9258*

*Corresponding Authors: Santiago Esplugas (e-mail: santi.esplugas@ub.edu) and Mohamed Gamal El-Din (e-mail: mgamalel-din@ualberta.ca)

Abstract

Combined sewer overflows (CSO), generated during the wet weather flow from the combination of the inflow and stormwater runoff in sewer system, result in an overflow of untreated wastewater from sewer system, which might ultimately contain different micropollutants (MPs). In this study, a coagulation-flocculation-sedimentation (CFS) pretreated CSO spiked with MPs was treated by catalytic ozonation using carbon, iron and peroxide based catalysts. The catalysts were characterized and their activity on MPs removal was studied at two different ozone (O_3) doses (5 and 10 mg L^{-1}). The effect of the treatment on the spiked CSO effluent was also assessed from the acute toxicity of the effluent using Microtox®, Yeast and Macrophage cell-line toxicity assay tests. All the carbon-based catalysts showed large surface area, which was strongly influenced by the activation technique in the preparation of the catalyst. The CFS treatment strongly reduced the turbidity (≥ 60%) but had marginal effect on the UV_{254}, dissolved organic

carbon (DOC) and pH. Sludge Based Carbon (SBC) showed strong adsorption capacity (≥ 60% removal efficiency) for all MPs studied compared to other carbon and iron-based catalysts. Ozonation alone was effective for the degradation of easily oxidizable MPs (sulfamethoxazole, mecoprop, and 2,4-dichlorophenoxyl acetic acid), achieving more than 80% degradation efficiency at 10 mg L^{-1} of ozone, but not effective for atrazine (≤ 60% degradation efficiency) at similar O_3 dose. Catalytic ozonation (at 10 mg L^{-1} O_3 dose) improved the degradation of the MPs at low catalyst dosage but higher dosage strongly inhibited their degradation. In all cases, the effluents showed negligible acute toxicity, indicating the suitability of the process for the treatment of CSO.

Keywords

Combined Sewer Overflows (CSO); catalytic ozonation; coagulation-flocculation-sedimentation (CFS); Micropollutants (MPs); Acute Toxicity

1. Introduction

In general, surface runoff from urban areas can be transported in separate sewer systems (*i.e.*, separated from sewage) or combined sewer systems (*i.e.*, combined with sewage). In a separate sewer system, stormwater is collected and discharged to the receiving water body or passed over stormwater management facilities. Combined sewer systems, on their part, are sewers that are designed to collect rainwater runoff, domestic sewage, and industrial wastewater in the same pipe. The total flow is transported to wastewater treatment plants (WWTP) where it is treated and then discharged to a water body. However, during heavy rainstorms a part of the total flow is diverted out of the sewer system to receiving waters at overflow structures. Otherwise, high water flows would exceed the sewer system or WWTP capacity. These overflows contain municipal sewage and are known as Combined Sewer Overflows (CSO). This type of waters may be highly polluted and usually are discharged without any treatment [Kumar Chhetri et al., 2014], causing environmental impacts to receiving systems. This is a common problem in cities in the United States and Canada, among other world regions where combined sewer systems are implemented. The negative consequences for the receiving aquatic ecosystems can range from short- to long-term type (bioaccumulation, eutrophication, fish mortality increment, low level of dissolved oxygen, etc.) [Riechel et al., 2020; Kumar Chhetri et al., 2016]. In any case, it is necessary to implement a back-up treatment system capable to treat CSO during heavy rainstorm events.

CSO can contain a large amount of organic matter, pathogens and micropollutants (MPs). MPs are recalcitrant and present in low concentrations in the environment [López-Vinent et al., 2020; López-Vinent et al., 2019; Richardson and Kimura]. They can enter in the aquatic ecosystem causing harmful ecological and human health effects [De la Cruz et al., 2012; Ortiz de García et al., 2013]. Conventional treatments (such as biological treatments) are not suitable to remove MPs due to the properties of these compounds [Ganiyu et al., 2015; López et al., 2017], and they are not designed for occasional applications. In order to protect the ecosystems and water resources, and in accordance with future law requirements, additional techniques are necessary to eliminate MPs. In this sense, chemical treatment appears as a good choice. In the last decades, a common alternative to conventional treatments has been the use of Advanced Oxidation Processes (AOPs). Among the different AOPs, ozonation seems to be one of the most cost-effective and easily implementable technologies to remove organic compounds from water and wastewater [Cruz-Alcalde et al., 2019a]. However, a pretreatment is necessary before the ozonation step in order to eliminate the large amount of organic matter present in CSO, including solids. A good removal of this organic matter can be achieved by chemical coagulation-flocculation [El Samrani et al, 2008].

Concerning ozonation, an extensive number of studies from laboratory to large-scale have reported the efficiency of ozone (O_3) application for MPs removal in wastewater effluents [Blackbeard et al., 2016; Bourgin et al., 2018; Cruz-Alcalde et al., 2019a; Chys et al., 2017; Dogruel et al., 2020; Mecha et al., 2016; Singh et al.]. Nevertheless, O_3 is a selective oxidant, which means that not all compounds can be removed with direct O_3 reaction [von Gunten, 2003]. However, the decomposition of O_3 in water matrices produces hydroxyl radical ($^{\bullet}OH$), which is a non-selective oxidant [von Gunten, 2003; Lee and von Gunten, 2009], with a high oxidative power. In order to enhance the natural formation of $^{\bullet}OH$ during wastewater ozonation, a promising strategy is the addition of catalysts and other reagents capable of reacting with ozone to yield $^{\bullet}OH$ [Li et al., 2008; Malvestiti et al., 2019; Zhu et al., 2017]. In particular, carbon-, iron- and peroxide-based materials have previously shown promising performances as potential catalysts in ozonation [Li et al., 2018; Rajah et al., 2019; Vatankhah et al., 2019; Yin et al., 2016; Ziylan and Ince, 2015]. Moreover, solid catalysts, especially carbon-based materials, can present additional advantages, regarding MPs removal, as adsorption. Studies reporting potential strategies for CSO treatments are scarce, and only a few works reported the use of O_3 and AOPs for

disinfection of this kind of waters [Wojtenko, 2001; Tondera et al., 2015]. To the best of our knowledge, no studies about MPs removal from CSO have been reported so far. The main goals of this study were i) to evaluate the efficiency of primary treatment for CSO water consisting of a first coagulation-flocculation-sedimentation step and subsequent O_3 oxidation, with the main goal of removing organic contaminants, ii) to test different oxidants and catalysts combined with ozone in order to determine alternatives for an enhanced primary treatment during wet weather flow and iii) to assess potential impacts of these treatment strategies on the biodegradability and acute toxicity of CSO .

2. Methodology

2.1. Chemicals and reagents

Sulfamethoxazole (SMX), mecoprop (MCP), atrazine (ATZ) and 2,4-dichlorophenoxy acetic acid (2,4-D) purchased from Sigma-Aldrich (Germany) were used as target compounds. These contaminants were selected according to their reactivity with O_3, as this parameter determines their degradation efficiency during the process. SMX is highly reactive with O_3 ($k_{SMX,O3} = 5.5 \times 10^5$ M^{-1} s^{-1} [Huber et al., 2003]), whereas MCP and 2,4-D both display medium reactivity (k_{O3} values of 111.0 M^{-1} s^{-1} [Beltrán et al., 1994] and 21.9 M^{-1} s^{-1} [Benitez et al., 2004], respectively). ATZ, on its part, is an ozone-resistant compound ($k_{ATZ,O3}$= 6 M^{-1} s^{-1}) [Acero et al., 2000]. Regarding $^{\bullet}OH$ reactivity, all compounds present high second-order rate constants with the radical (values of 5.5×10^9 M^{-1} s^{-1} [Huber et al., 2003], 9.1×10^9 M^{-1} s^{-1} [Beltrán et al., 1994], 5.1×10^9 M^{-1} s^{-1} [Benitez et al., 2004] and 3×10^9 M^{-1} s^{-1} [Lee and von Gunten, 2009] for SMX, MCP, 2.4-D and ATZ, respectively). Granular Activated Carbon (GAC), zero valent iron (ZVI), magnetite (Fe_3O_4), peracetic acid (PAA), hydrogen peroxide (H_2O_2, 30% *w/w*), ferrous sulfate ($FeSO_4 \cdot 7H_2O$) were tested as catalysts or oxidants in combination with O_3. They were all also purchased from Sigma-Aldrich. Aluminium sulphate ($Al_2(SO_4)_3$), acquired from Sigma-Aldrich (USA), was used in the coagulation-flocculation process. For HPLC determinations, Milli-Q® water and acetonitrile (Fisher, USA) were used as mobile phases. Sodium bisulfite ($NaHSO_3$) was employed as quencher of H_2O_2 and PAA in H_2O_2/O_3 and PAA/O_3 oxidation experiments.

2.2. Combined Sewer Overflows and coagulation-flocculation-sedimentation treatment

CSO water used in this study was simulated by mixing one part of primary effluent of a WWTP in the city of Edmonton (Alberta, Canada) (obtained during dry weather conditions) and one part of deionized water (50:50). A pretreatment based on coagulation-flocculation-sedimentation (CFS) was firstly performed on CSO water to enhance the subsequent ozone-based oxidation processes. In brief, 2 L of simulated CSO were placed in glass containers equipped with mechanical stirring, that is, a jar-test device (PB-700 Jartester, Phipps & Bird, USA). A concentration of 75 mg L^{-1} of $Al_2(SO_4)_3$ was added, and immediately a fast stirring regime (1500 rpm) was firstly applied for 1 min, followed by slow stirring at 150 rpm for 30 min. Finally, the agitation was turned off, and after 1 h of settling the supernatant was taken to conduct oxidation experiments [Alameddine, et al., 2020].

2.3. Ozonation experiments

Adsorption, ozonation and catalytic ozonation experiments were performed in 30 mL vials containing simulated CSO, after CFS, and spiked with 1 mg L^{-1} of each target compound (SMX, MCP, 2,4-D and ATZ, mixed simultaneously). The pH of the solution was the natural pH (7.5) of CSO matrix. O_3 was generated from pure oxygen by means of a GSO-30 ozone generator (Wedeco, USA). O_3 stock solutions were prepared by bubbling an O_2/O_3 gaseous mixture in Milli-Q water cooled in an ice bath. The resulting O_3 concentrations of these solutions were ~ 1 mM. In the case of O_3 combined with catalysts and other oxidants, the latter were added at the solution just before the O_3 dosage. Two O_3 doses (5 and 10 mg O_3 L^{-1}) were selected to perform the experiments based on literature, as these doses can be regarded as typical treatment conditions in ozone-based processes [Lee et al., 2013]. The catalyst dosages selected for ZVI, Fe_3O_4 and carbon-based catalysts were 50, 100 and 500 mg L^{-1}. In the case of homogeneous catalysts, different concentrations were chosen depending on each case. Thus, in the case of H_2O_2 and PAA three ratios related to the following O_3 molar concentrations (*i.e.*, peroxide/O_3) were selected: 0.25, 0.5 and 1, as these are common ratios discussed in literature [Cruz-Alcalde et al., 2019b]. The concentrations of iron (II) in the case of O_3/Fe^{2+} experiments were 1, 5 and 10 mg L^{-1} Fe^{2+}. All experiments were performed for 30 min (time required for total consumption of selected O_3 doses) and the vials were constantly shacked. Samples were filtered with 0.25 μm PVDF filters prior to analysis. In the experiments with PAA and H_2O_2, the samples were quenched with $NaHSO_3$. All experiments were performed in duplicate and average value was reported. Adsorption

experiments were also carried out as controls at similar experimental conditions in the absence of O_3.

The information about the preparation of the carbon-based catalyst and the characterization of all catalysts investigated in this study can be found in Text S1-S2 of supplementary material.

2.4. Analytical methods

Ultrospec 2100 UV-Visible Spectrophotometer (Biochrom, USA) was used to measure the UV absorption and standardize the O_3 stock solutions. The Indigo method [Bader and Hoigné, 1981] was also employed for dissolved O_3 measurements. MPs were detected using an Infinity Series HPLC of Agilent coupled with UV/Vis detector. A Zorbax Eclipse XBD C18 (150 × 4.6 mm i.d; 5 μm particle size) was the employed column. Acetonitrile (A) and Milli-Q water adjusted to pH = 3 by orthophosphoric acid (B) were employed as mobile phases. The analyses were performed under a gradient method as follows: 30% A and 70% B initially kept for 5 min, 30% A to 60% A during 5 min, 60% A and 40% B kept for 25 min, 60% A to 80% A during 5 min, 80% A and 20% B kept for 30 min, 80% A to 30% A during 10 min and finally 30% A and 70% B kept for 10 min. Total organic carbon (TOC) was determined using a TOC-V CNS Total Organic Carbon analyzer by Shimadzu (Japan).

3. Results and discussion

3.1. CSO pretreatment

CFS pretreatment was performed in order to enhance the subsequent catalytic ozonation. Table 1 lists the characteristics of the CSO before and after the CFS process. El-Samrani and coworkers [El Samrani et al., 2008] studied the physicochemical characteristics of CSO corresponding to a weak rain and storm event, with turbidity values of 44.8 and 114 NTU, respectively. In storm events, typical values of turbidity are high (114 NTU in their study) and from weak rain episode the values of turbidity are much lower (44.8 NTU from their study). In the present study, the turbidity of simulated CSO before CFS was 33.6 NTU, which could be associated to a weak rain event. After the CFS pretreatment, turbidity decreased by 61% (13.2 NTU). A similar trend was followed by DOC, with an observed drop of 27% after the CFS treatment. The value of pH was very close before and after the CFS, and 20% reduction of UV_{254} was achieved, giving a rough idea of the remaining aromatic character of the water effluent.

Table 1. Characteristics of the final CSO effluents before and after coagulation-flocculation-sedimentation. (Before spike the MPs).

Parameter	Before CFS	After CFS
pH	7.5	7.6
Turbidity (NTU)	33.6	13.2
UV_{254} (cm^{-1})	0.20	0.16
DOC (mg C L^{-1})	23.0	16.7

3.2. Ozone-based oxidation treatments

3.2.1. Catalysts adsorption capacities for the MPs

Fig. 1 presents the adsorption of the selected MPs (ATZ, SMX, 2,4-D and MCP) on the carbon-based materials and ZVI for three different catalyst dosages (50, 100 and 500 mg L^{-1}). All experiments were performed using MPs spiked CFS pretreated CSO and continuously shacked for the duration of 30 min. These tests were carried out to evaluate the adsorption capacity of the carbon-based and solid Fe-based catalysts for the MPs and take this into consideration when determining the catalytic activity of these catalysts during catalytic ozonation treatment. For Fe_3O_4, Fe^{2+} and peroxide-based materials, blank tests were also performed. However, neither MPs degradation nor adsorptions were observed when these were tested without O_3.

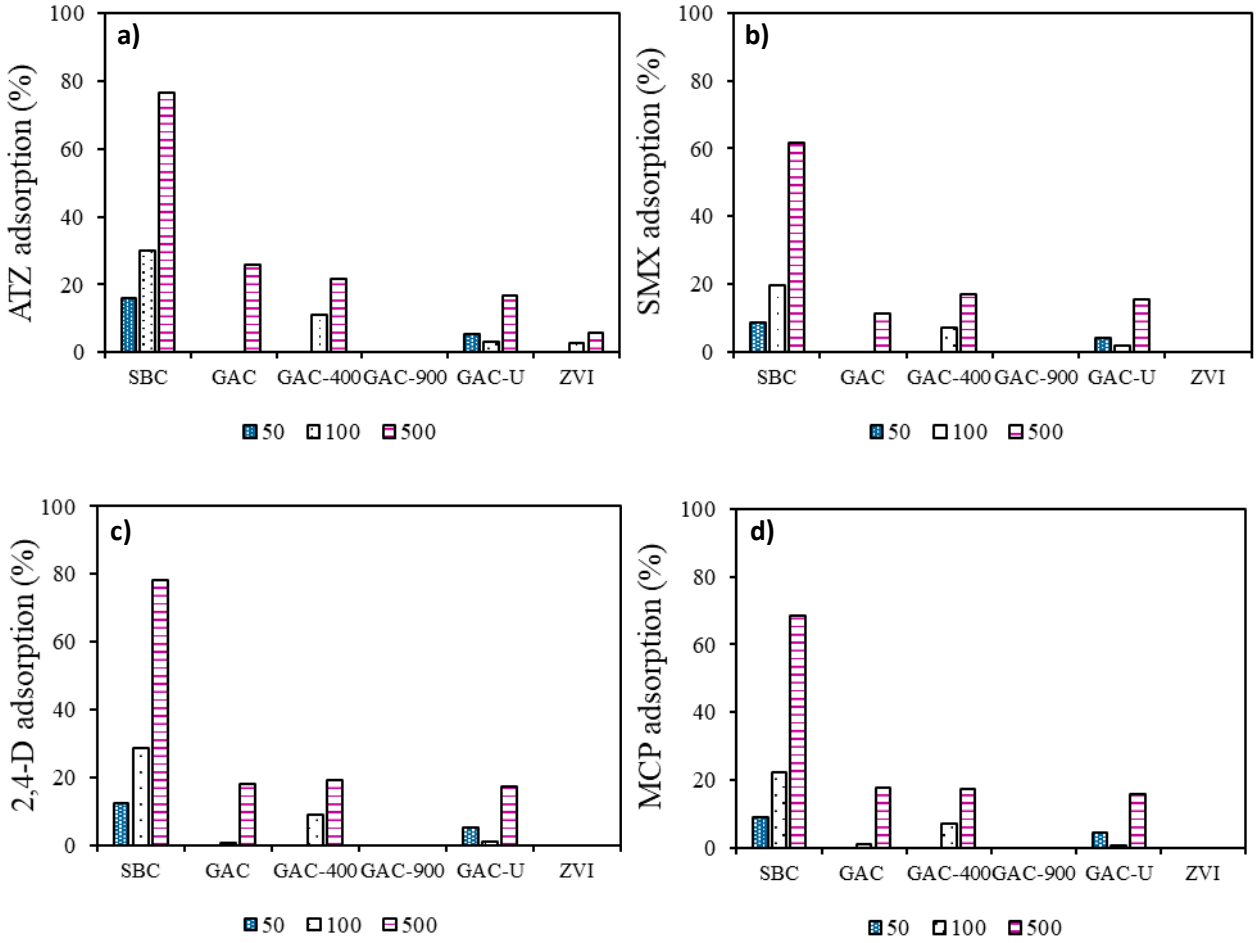

the 30 min adsorption test using 50, 100 and 500 mg L^{-1} catalyst dosage.

As observed in Fig. 1, major adsorptions for all MPs took place onto SBC. These results are in accordance to textural properties detailed in supplementary material (Text S6, Text S7, Table S2, Table S3 and Figure S1). As can be seen in Table S2, SBC presented more mesopores than the other carbon-based catalysts and the highest V_{micro}/V_{total} ratio (0.16). Therefore, the presence of a higher number of mesopores was the reason behind the observed highest adsorption capacity. Additionally, the lower treatment temperature and the precursor for the SBC gives the catalyst many surface functional groups, which aided the adsorption of the pollutants. Concerning GAC and their derivatives, it was observed that the increase in the material treatment temperature directly impacted the adsorption capacity of these materials. GAC-900, which was treated at 900 ºC, did not present adsorption at any dosage for any of the micropollutant, even with its highest surface area. This can be attributed to the high temperature treatment, which liberates most of the surface functional groups that may serve as adsorption site in the catalyst. However,

GAC-400, which was treated at 400 ºC, exhibited similar adsorption performance than GAC. GAC-U showed slightly low adsorptions for the three tested dosages, contrarily to GAC which only presented adsorption for a dose of 500 mg L^{-1}. ZVI presented very low adsorptions and were only noticeable in the case of ATZ for 100 and 500 mg L^{-1} (3 and 6%, respectively).

Regarding catalysts dosage, as expected, the higher the dosage the greater the observed adsorption of the MPs. For instance, in SBC, ATZ removal efficiency was 15.84, 30.08 and 76.44 % for 50, 100 and 500 mg L^{-1}, after 30 min of treatment, demonstrating the increase in adsorption sites and capacity with increased catalyst dosage.

The differences observed, between the four selected MPs in the removal efficiency by the catalysts, can be associated to the different adsorption mechanisms of the MPs and their physicochemical properties. Nevertheless, SMX presented the lowest adsorption, which was well appreciated in the case of SBC material. These results are in accordance to the relative polarity of the different MPs, typically expressed in terms of the log K_{ow} (octanol-water partition coefficient) value. Thus, log K_{ow} values for ATZ, SMX, 2,4-D and MCP are 2.61, 0.89, 2.81 and 3.13, respectively. SMX presents the lowest log K_{ow} in agreement with its lowest adsorption.

3.2.2. Catalytic ozonation using carbon-based catalysts

SBC, GAC, GAC-400, GAC-U and GAC-900 were used for the catalytic ozonation of the four selected MPs (see Figs. 2-6). Two O_3 concentrations were tested: 5 and 10 mg L^{-1}, as previously mentioned.

Single ozonation experiments with the same oxidant doses were also performed for comparison purposes, and results of catalytic experiments were presented discounting the adsorption in order to see better the catalytic effect. The employment of 10 mg L^{-1} of O_3 in single ozonation produced an improvement of MPs degradation compared to adsorption. This enhancement was mostly seen in ATZ, 2,4-D and MCP. However, 5 mg L^{-1} of O_3 were enough to achieve complete degradation of SMX. This fact is explained by the kinetics of the reaction of each compound with O_3. SMX presents the highest reactivity with O_3. On the other hand, ATZ displays a poor reactivity, whereas 2,4-D and MCP show medium reactivity. For instance, 26, 100, 49 and 60% degradation efficiency were achieved for ATZ, SMX, 2,4-D and MCP, respectively, with 5 mg L^{-1} of O_3. While

using 10 mg L^{-1} of O_3, the degradation efficiency was 56, 100, 83 and 93%, respectively at similar reaction time.

Regarding SBC (Fig. 2), no catalytic activity was observed, and in fact the removal of MPs due to the combination of both agents (*i.e.*, ozonation and adsorption on SBC) decreased as the catalyst concentration increased. This may imply that there is quenching and scavenging of the O_3 by the SBC catalyst. Nevertheless, if the contribution of both adsorption and ozonation is considered, treatment of MPs spiked CSO at 10 mg L^{-1} O_3 dose showed better removal of MPs at all SBC dosages compared to treatment at 5 mg L^{-1} O_3 dose, even though the observed MPs removal efficiency was all due to the adsorption. This fact was explained in section 3.2.1 and related to textural properties of SBC as well as its surface functional groups.

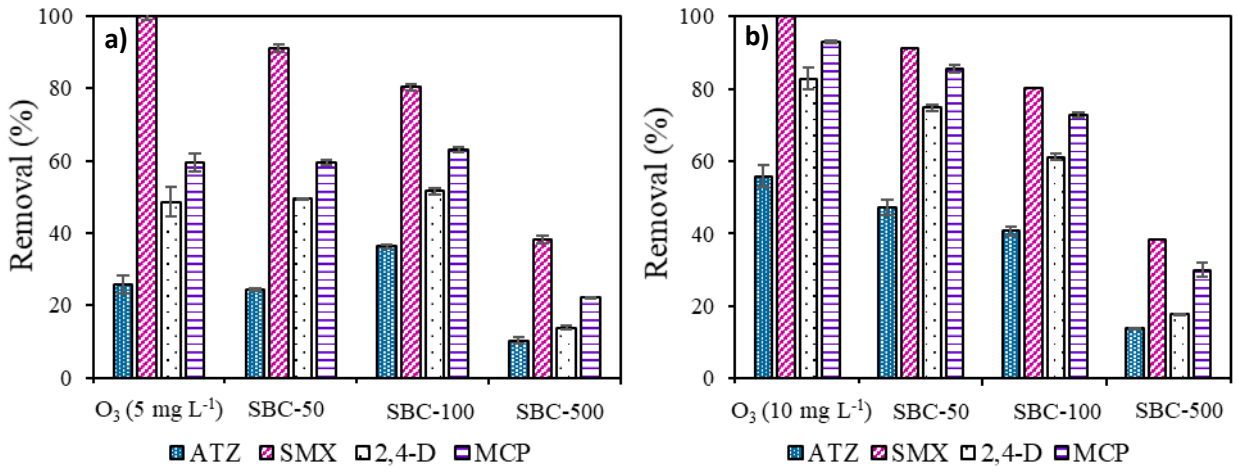

Figure 2. Catalytic activity (without adsorption) of SBC with (a) 5 mg L^{-1} and (b) 10 mg L^{-1} doses of O_3 for three catalyst dosages (50, 100 and 500 mg L^{-1}) and for each MP degradation in CSO.

Results corresponding to experiments with commercial GAC and their derivatives as catalysts are shown in Fig. 3. Contrary to SBC, GAC did not display a high adsorption capacity. Only when highest commercial GAC dose (500 mg L^{-1}) was tested, 10-25% MPs removal efficiency due to adsorption were observed, ATZ being the highest adsorbed compound (26%) and SMX the lowest one (11%). A positive enhancement was observed in ATZ removal with 100 mg L^{-1} dose, being 11 and 9% higher (Fig. 3a and 3b) in the case of catalytic ozonation than in single ozonation (for O_3 doses of 5 and 10 mg L^{-1}, respectively). However, the sum of adsorption and oxidation in ATZ promoted high removal when 500 mg L^{-1} of GAC was tested. The degradation efficiencies for catalytic

ozonation (5 and 10 mg L^{-1} of O_3) were 50 and 72%, (Fig. 4a and 4b) respectively, versus 26 and 56% for single ozonation.

In catalytic ozonation, GAC not only acts as an adsorbent, but also as a catalyst increasing the decomposition of O_3 to $^{\bullet}OH$ via hydroperoxyl radical formed in the reaction of O_3 with pyrrole group at graphene layer of GAC (Eqs. (1-4)) [Sanchez-Polo et al., 2005].

$$HO_2^{\bullet} \leftrightarrow O_2^{\bullet-} + H^+ \quad (1)$$

$$O_3 + O_2^{\bullet-} \rightarrow O_3^{\bullet-} + O_2 \quad (2)$$

$$O_3^{\bullet-} + H^+ \rightarrow HO_3^{\bullet} \quad (3)$$

$$HO_3^{\bullet} \rightarrow {}^{\bullet}OH + O_2 \quad (4)$$

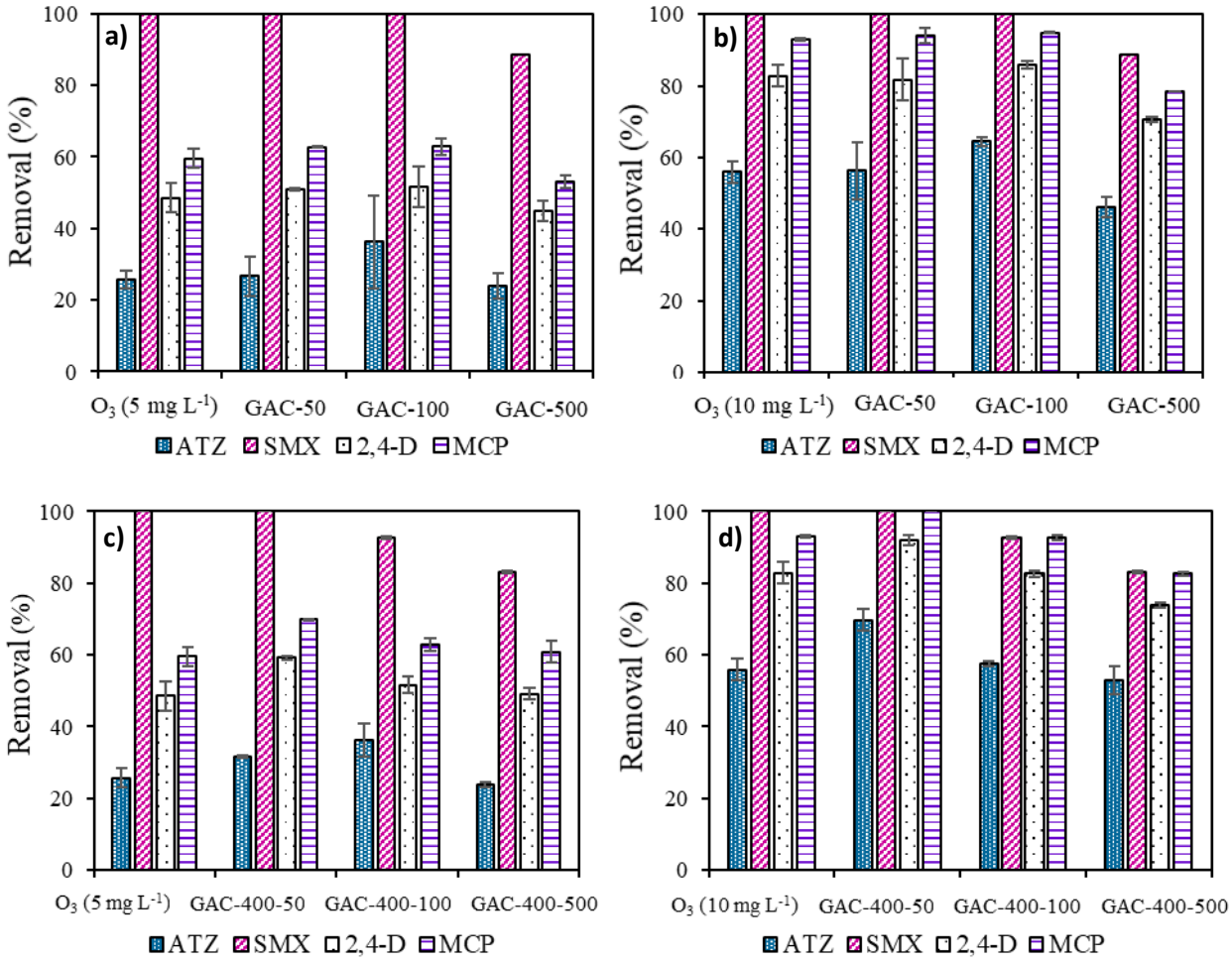

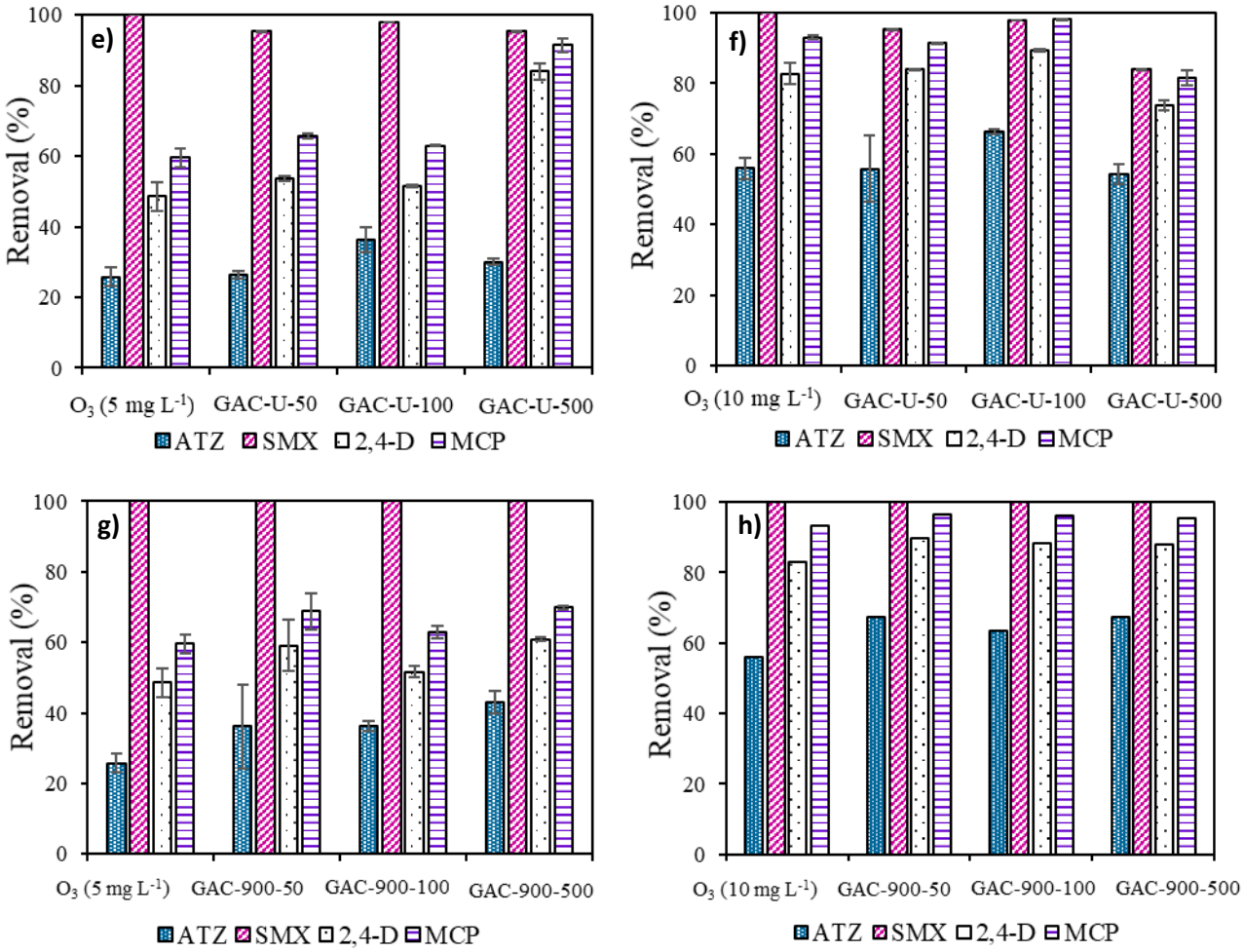

Figure 3. Catalytic activity (without adsorption) of (a,b) GAC, (c,d) GAC-400, (e,f) GAC-U (g,h) GAC-900 with (a,c,e,g) 5 mg L^{-1} and (b,d,f,h) 10 mg L^{-1} O_3 doses for three catalytic dosages (50, 100 and 500 mg L^{-1}) and for each MP degradation in CSO.

Among the derivatives of GAC, GAC-400 and GAC-U showed the best performances compared to commercial GAC (see Figs. 3c and 3d, and 3e and 3f). For instance, for ATZ removal, using 5 mg O_3 L^{-1} and 50 mg L^{-1} of catalyst, the degradations (oxidation + adsorption) were: 27, 32 and 41 % for GAC, GAC-400 and GAC-U, respectively. In the case of GAC-U there was a slight adsorption of ATZ (~ 4%). For the other catalysts, no adsorption was observed in these experimental conditions. Even though there was adsorption, the use of GAC-U as catalyst showed a high removal of MPs by oxidation or by an improvement of the adsorption capacity of the catalyst upon surface oxidation by O_3 and/or $^{\bullet}OH$.

When 100 mg L^{-1} of catalysts was used, in all cases the oxidation was higher than adsorption. However, for the highest dose of catalysts (500 mg L^{-1}), a curious fact was observed. For GAC-400 and commercial GAC, the removal of MPs by oxidation or adsorption was balanced, presenting similar results by both catalysts (24% of oxidation and adsorption). When GAC-U was tested (500 mg L^{-1}), 43% and 15.70% of ATZ removal were registered for oxidation and adsorption, respectively. These differences were probably due to the nitrogen incorporated in GAC-U, which apparently increased the reactivity of the GAC surface towards O_3, enhancing the yield of $^{\bullet}OH$. This agrees with the highest basicity of GAC-U (pH_{pzc}= 8.1, *i.e.*, the highest value among all tested catalysts), which in turn could be associated to a larger presence of electron-donating moieties at its surface.

GAC-900 did not exhibit any adsorption capacity in the range of dosage tested. The results of oxidation are shown in Fig. 3g and 3h and were similar compared to GAC. Thus, no improvement was seen from the commercial catalyst. GAC-900 was treated at 900 ºC and this high temperature probably caused the removal of acidic and basic functional groups from the catalyst surface [Figueiredo et al., 1999]. The elimination of acidic groups on the catalyst surface may enhance the reactivity of the material with O_3 and probably the production of $^{\bullet}OH$, as acidic groups tend to be more electronegative than basic groups [Figueiredo et al., 1999]. This fact was observed for GAC-400 and GAC-U. However, in GAC-900, the removal of basic groups also took place because of high temperature, eliminating the potential positive effect and leading to similar results than those observed in experiments with commercial GAC.

Besides the previous reasons for the low removals of MPs, this behavior was also caused by the complexity of the matrix. The EfOM (Effluent organic matter) contained in the CSO can also react with the O_3 and only a small part of that is available for the catalysts to generate $^{\bullet}OH$. Moreover, this organic matter can be adsorbed by the catalysts, saturating their pores and decreasing the efficiency to react with the O_3.

3.2.3. *Catalytic ozonation using Iron-based catalyst*

ZVI, Fe_3O_4 and Fe^{2+} were used as a catalyst combined with O_3 (see Fig. 4). The same concentrations of O_3 than those used in carbon-based catalytic experiments were tested (5 and 10 mg L^{-1} O_3 doses). Regarding the catalytic experiments with ZVI (Fig. 4a and 4b), slight differences were observed compared to single ozonation (see 3.2.1). The

highest improvement was an increase from 26 to 36% in the removal of ATZ, achieved by using 100 mg L^{-1} of ZVI and 5 mg L^{-1} of O_3. Again, this is explained by the poor reactivity of ATZ with O_3. In catalytic ozonation, the reaction between catalyst and O_3 is expected to enhance the natural generation of $^{\bullet}OH$, which is not selective and can easily oxidize ATZ ($k_{OH,ATZ}$ = 3.00 × 10^9 M^{-1} s^{-1} vs $k_{O3,ATZ}$= 6 M^{-1} s^{-1}).The employment of different catalyst dosages did not achieve significant differences. For example, in the case of ATZ abatement with 5 mg L^{-1} of O_3, the removals were 33, 36 and 24% for 50, 100 and 500 mg L^{-1}, respectively. The increase in removal efficiency was only 4%, raising from 50 to 100 mg L^{-1} ZVI. However, the ATZ removal using 500 mg L^{-1} of ZVI was similar than single ozonation, indicating that higher catalyst dosage does not necessarily trigger a positive effect in catalytic ozonation with ZVI.

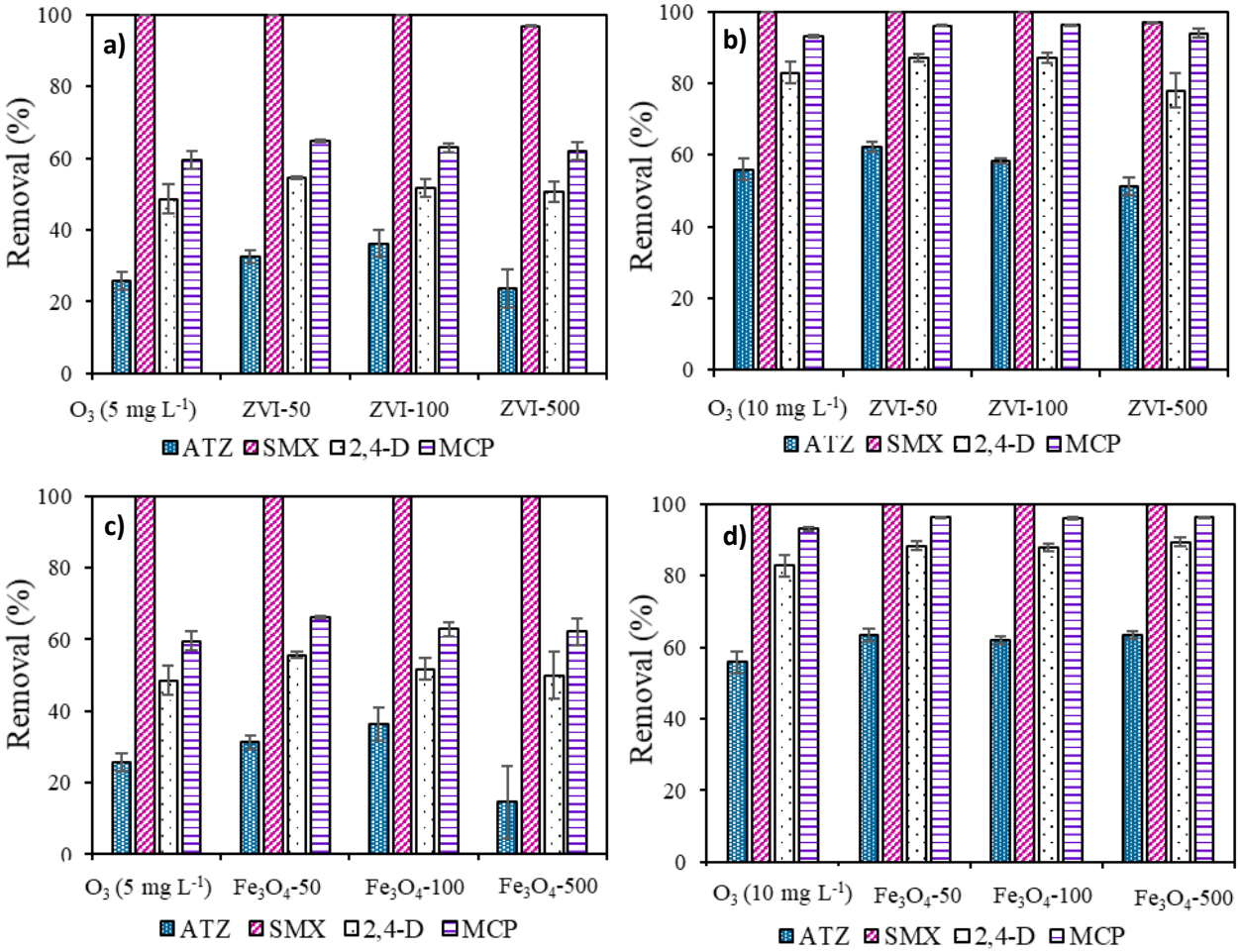

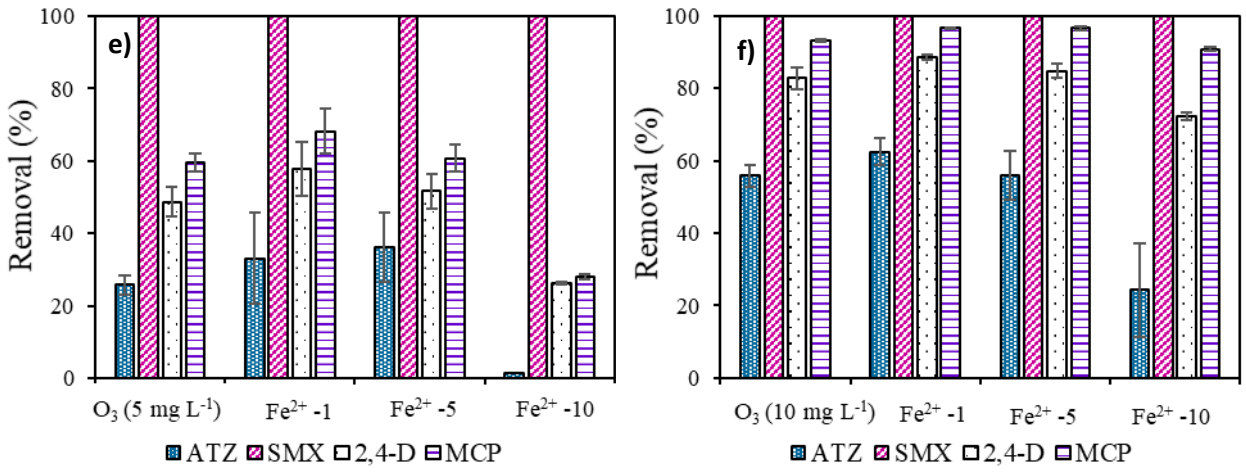

Figure 4. Catalytic activity (without adsorption) of (a,b) ZVI, (c,d) Fe_3O_4 and (e,f) Fe^{2+} with (a,c,e) 5 mg L^{-1} and (b,d,f) 10 mg L^{-1} O_3 doses for (a,b,c,d) three catalyst dosages of ZVI and Fe_3O_4 (50, 100 and 500 mg L^{-1}) and (e,f) three concentrations of Fe^{2+} (1, 5 and 10 mg L^{-1}) for each MP degradation CSO.

Fe_3O_4 was also tested as potential catalyst. Fig. 4c and 4d shows the removals (%) for ATZ, SMX, 2,4-D and MCP with 5 and 10 mg L^{-1} of O_3. Comparing these data with those obtained when using ZVI, similar results were achieved with different doses of catalyst and MPs. The most probable explanation to this relatively poor performance of these catalysts is the fact that reactions of both Fe_3O_4 and ZVI with O_3 are slow [Ziylan and Ince, 2015]. Moreover, it also has to be taken into account that CSO present high DOC, which is typically the main sink of $^{\bullet}OH$ formed in AOPs.

No significant differences were seen with the increase of dosage from 50 to 100 mg L^{-1} of Fe_3O_4. The highest difference was found in the case of ATZ removal (5 mg L^{-1} of O_3), with an additional 5% of abatement (Fig. 4c). However, in other cases, such as in 2,4-D or MCP (at 5 mg L^{-1} of O_3), raising the catalyst dosage caused the decrease in the percentage of degradation (4 and 3% lower with 100 mg L^{-1} for 2,4-D and MCP, respectively). A negative effect was also seen when 500 mg L^{-1} of Fe_3O_4 were used for ATZ removal with 5 mg L^{-1} of O_3. In that case, the degradation was even lower than single O_3 (15 and 26% for 500 mg L^{-1} of Fe_3O_4 and single O_3, respectively). However, with 10 mg L^{-1} O_3 dose, similar degradation efficiency of MPs was achieved at all catalyst dosages studied. In essence, the use of solid iron-based catalyst in excess of 50 mg L^{-1} for catalytic ozonation either had no significant impact on or reduced the degradation efficiency of the MPs at both O_3 doses studied. This can be attributed to (i) aggregation

457 of the ZVI and Fe_3O_4 particles due to their strong magnetic properties, thus reducing the
458 active surface area and catalytic sites for the activation of the O_3 to $^{\bullet}OH$ and (ii)
459 scavenging effect of excess catalyst on the $^{\bullet}OH$ since it is non-selective oxidant.

460 Compared to single ozonation, the highest difference was, similarly to that observed when
461 employing ZVI as catalyst, in ATZ removal. An extra 11% abatement was achieved with
462 catalytic ozonation in contrast with only O_3 (100 mg L^{-1} of Fe_3O_4 and 5 mg L^{-1} of O_3).
463 As can be observed, these differences were higher with 5 mg L^{-1} compared to 10 mg L^{-1}
464 of O_3. As commented before, the complexity of the matrix, which contains different types
465 of organic matter, strongly influences the MPs degradation. When low concentration of
466 ozone is used, a high fraction of ozone is consumed by the organic matter present in CSO.
467 However, when 10 mg·L^{-1} of O_3 are used, a lesser amount of the oxidant is consumed by
468 the background organic matter, and then its availability to remove MPs is higher than that
469 when using 5 mg L^{-1} of O_3. Thus, the MPs degradations were higher with 10 mg L^{-1} O_3
470 but the effect of adding a catalyst is more noticeable when employing the low O_3 dose .

471

472 Fe^{2+} was also tested as iron-based homogeneous catalyst. Fig. 4e and 4f show the
473 removals (%) for ATZ, SMX, 2,4-D and MCP with 5 or 10 mg L^{-1} of O_3. In this case, the
474 concentrations tested were 1, 5 and 10 mg L^{-1} of Fe^{2+}. The enhancement in MPs removal
475 compared to single ozonation was more noticeable than that observed when using solid
476 iron-based catalysts, especially in the case of low and medium reactive MPs and iron
477 concentrations of 1 and 5 mg L^{-1}. This can be explained by the faster activation of O_3 to
478 $^{\bullet}OH$ by the homogeneous Fe^{2+} ions due to the proximity of the O_3 to Fe^{2+} ions in the
479 homogeneous solution. The aqueous phase of both reactants enhanced the reaction rate
480 compared to the reaction between O_3 with ZVI and Fe_3O_4 which are heterogenous solid
481 catalysts. Additionally, there was no aggregation of catalysts in this case of Fe^{2+} as was
482 observed with ZVI and Fe_3O_4. However the removals of these compounds dramatically
483 decreased, when 10 mg L^{-1} of Fe^{2+} were used. This can be explained by the oxidation of
484 Fe^{2+} by ozone to yield Fe^{3+} (Eqs. (4-6)), followed by precipitation of iron in the form of
485 Fe(III) hydroxide. Formation of this precipitate was in fact observed during the
486 experiments, especially when employing higher initial concentrations of Fe^{2+}.
487 Additionally, the observed performance decrease can be attributed to the scavenging
488 effect of the excess Fe^{2+} (Eq. (9)), which quenched the $^{\bullet}OH$ generated from the activation
489 of O_3. The scavenging effect of excess Fe^{2+} in Fe-catalyzed AOPs such as Fenton and

related processes are well studied [Brillas et al., 2009; Ganiyu et al., 2018]. The mechanisms of activation of O_3 by Fe^{2+} ions in catalytic ozonation are summarized in Eqs. (5-12) and they involve the generation of ozonide ($O_3^{\bullet-}$) and $^{\bullet}OH$, which are responsible of the MPs degradation in the O_3/Fe^{2+} system [Beltran et al., 2005].

$$Fe^{2+} + O_3 \rightarrow Fe^{3+} + O_3^{\bullet-} \quad (5)$$

$$Fe^{2+} + O_3 \rightarrow FeO^{2+} + O_2 \quad (6)$$

$$FeO^{2+} + H_2O \rightarrow Fe^{3+} + {}^{\bullet}OH + OH^- \quad (7)$$

$$Fe^{3+} + O_3 \rightarrow FeO^{2+} + H^+ + {}^{\bullet}OH + OH^- \quad (8)$$

$$Fe^{2+} + {}^{\bullet}OH \rightarrow Fe^{3+} + OH^- \quad (9)$$

$$Fe^{2+} + FeO^{2+} + 2H^+ \rightarrow 2Fe^{3+} + H_2O \quad (10)$$

$$Fe^{2+} + HO_2^{\bullet} \rightarrow Fe^{3+} + HO_2^- \quad (11)$$

$$Fe^{3+} + HO_2^{\bullet} \rightarrow Fe^{2+} + H^+ + O_2 \quad (12)$$

3.2.4 Peroxide- ozonation treatments

H_2O_2 and PAA were also tested with O_3. The ratios (mg oxidant / mg O_3) employed to perform the experiments were 0.25, 0.5 and 1. Blank tests with only H_2O_2 or PAA were performed and no MPs removal was observed in any case. The results are depicted in Fig. 5a and 5b, and 5c and 5d for H_2O_2 and PAA, respectively. As can be observed in Fig. 5a and 5b, the ratio H_2O_2/O_3 does not has influence on the ATZ removal with 5 mg L^{-1} O_3 dose (34, 33 and 35% for 0.25, 0.5 and 1 ratio, respectively) (Fig. 6a). The same trend was observed when 10 mg L^{-1} O_3 were used with similar degradation efficiency observed for each MP at different ratios studied. The highest improvement in MPs degradation efficiency during H_2O_2/O_3 treatments compared to single ozonation were around 8% and 13% for 5 and 10 mg L^{-1} O_3, respectively. These low enhancements are caused by the EfOM present in the CSO, as explained above. The consumption of ozone is mainly controlled by its reaction with EfOM, and not by the reaction with H_2O_2. Thus, only a small part of O_3 is available to react with H_2O_2 to form $^{\bullet}OH$. The mechanisms of peroxone are described by reactions in Eqs. (13-21). In addition, the decomposition of ozone can

519 be initiated by hydroxide anion but, in wastewater ozonation, this mechanism is negligible
520 due to the EfOM present in wastewater, as explained above [Cruz-Alcalde, et al. 2019b].

521 $O_3 + HO_2^- \rightarrow HO_5^-$ (13)

522 $HO_5^- \leftrightarrow HO_2^\bullet + O_3^{\bullet-}$ (14)

523 $HO_5^- \rightarrow 2O_2 + OH^-$ (15)

524 $HO_2^\bullet \leftrightarrow O_2^{\bullet-} + H^+$ (16)

525 $O_3 + O_2^{\bullet-} \rightarrow O_3^{\bullet-} + O_2$ (17)

526 $O_3^{\bullet-} \leftrightarrow O^{\bullet-} + O_2$ (18)

527 $O^{\bullet-} + H_2O \leftrightarrow {}^\bullet OH + OH^-$ (19)

528 ${}^\bullet OH + O_3 \rightarrow O_2 + HO_2^\bullet$ (20)

529 $H_2O_2 + {}^\bullet OH \rightarrow HO_2^\bullet + H_2$ (21)

530
531
532
533
534
535
536
537
538
539
540
541
542
543
544
545
546
547

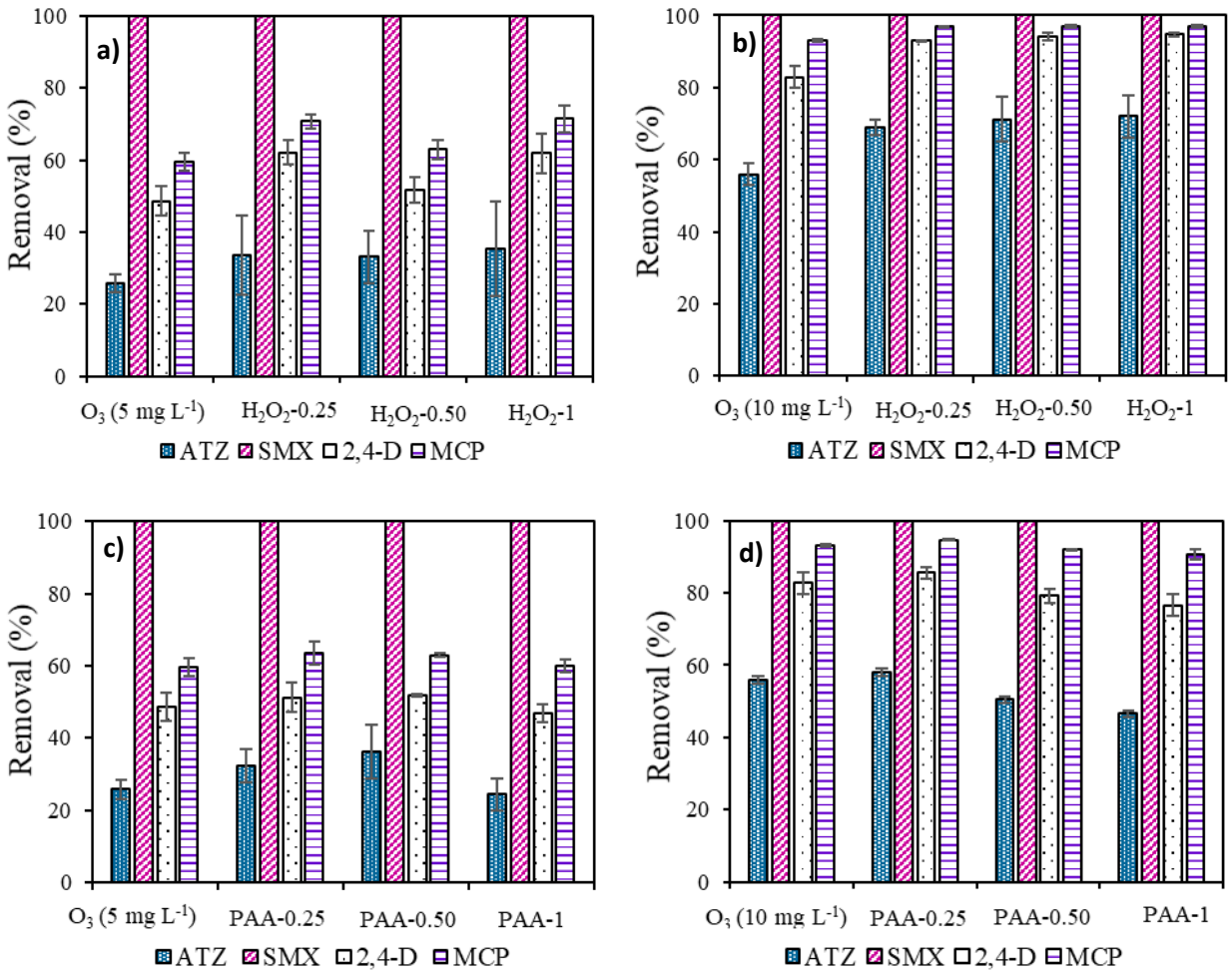

Figure 5. Catalytic activity (without adsorption) of (a,b) H_2O_2 (c,d) PAA with (a,c) 5 mg L^{-1} and (b,d) 10 mg L^{-1} O_3 doses for three ratios (0.25, 0.5 and 1) (H_2O_2 or PAA)/O_3 (mg/mg) for each MP degradation in CSO.

Fig. 5c and 5d shows the MPs degradation for PAA-ozonation treatments. In this case, the lower ratio (0.25) presented the best degradation efficiency of the MPs whereas, a higher ratio (0.5 or 1) achieves either similar (0.5 PAA with 5 mg L^{-1} O_3) or a lower MPs degradation. This behavior is due to the fact that PAA is an organic compound and can acted as scavenger for •OH. Taking into account the value of pK_a (8.2) [Luukkonen and Pehkonen, 2017] and the constants for the reaction of •OH with deprotonated PAA (PAA^-) ($k_{PAA^-, \bullet OH} = 9.33 \times 10^8$ $M^{-1}s^{-}1$) and neutral species (PAA^0) (pH 3-7) ($k_{PAA^0, \bullet OH} = 9.97 \times 10^9$ $M^{-1}s^{-1}$) [Meiquan et al., 2017], the $k_{PAA, \bullet OH}$ of reaction between •OH and PAA at pH 7.5 (pH of the solution) was calculated to be 2.44×10^9 $M^{-1}s^{-1}$. However, the value of the rate constant ($k_{H_2O_2, \bullet OH}$) of the reaction of H_2O_2 with •OH is 2.7×10^7 $M^{-1}s^{-1}$, which is lower than that of PAA [Meiquan et al., 2017].

578 Comparing the results achieved when ratio of 0.25 was tested at 5 mg L^{-1} O_3 dose with
579 peroxone and PAA-ozonation treatments, these were similar for ATZ degradation but
580 with peroxone process achieved better degradation efficiency for 2,4-D and MCP (11 and
581 7% higher for 2,4-D and MCP, respectively) compared to PAA-ozonation. In contrast,
582 at 10 mg L^{-1} O_3 dose, peroxone achieved better degradation efficiency for ATZ, 2,4-D
583 and MCP at all ratios studied compared to PAA-ozonation.

584 *3.4. Toxicity and biodegradability*

585 Toxicity assessments of treated CSO were performed for catalysts with the best MPs
586 removals during the catalytic ozonation treatment. One catalyst from each class of
587 materials was selected (Fe_3O_4, GAC-400 and H_2O_2) and used for the treatment of MPs
588 spiked CFS pretreated CSO. The effluents were collected for each treatment conditions,
589 filtered and used for toxicity experiments. To perform the analysis, the experimental
590 conditions chosen were 50 mg L^{-1} of Fe_3O_4 and GAC-400, ratio H_2O_2/O_3 0.25 and 10 mg
591 L^{-1} of O_3 dose. Single ozonation was also included at the same O_3 dose.

592 When new remediation techniques or catalysts were tested in real water, different toxicity
593 assays have to be performed due to the different sensitivity of each analysis. These
594 different toxicological studies allow the evaluation of the toxicity of final effluent more
595 precisely. In this work, biodegradability, Microtox with *Vibrio Fischeri*, mammalian cell
596 line toxicity and YES tests were performed. More information about these analyses can
597 be found in supplementary material (see Text S3-S5).

598 The results of Microtox toxicity, displayed in Fig. 6, were shown as percentage inhibition
599 of bioluminescence of V. *fischeri* bacteria after 5 and 15 minutes of exposure to the
600 samples. For 5 minutes of cell contact the effect was always lower than for 15 minutes.
601 Bigger differences were observed when oxidative treatments were carried out. In those
602 cases, especially when applying single ozonation and ozonation catalyzed by by GAC-
603 400, slightly higher toxicity was observed compared to the other measurements. Probably,
604 the differences in the % inhibition, when treatment was applied, were due to the
605 intermediate products formed when target MPs were degraded. The oxidation of most
606 MPs usually leads to the formation of organic intermediates, which in some cases are
607 more toxic than the parent compound. However, in case of single ozonation, GAC-400
608 and Fe_3O_4 catalyzed ozonation, the % inhibition was less than 10%, which means that
609 none of final effluent was significantly toxic to *V. fischeri*. In contrast, MPs spiked CFS

pretreated CSO treated by H_2O_2-ozonation (results not shown) exhibited complete (100 %) inhibition of *V. fischeri*, which was due to the residual H_2O_2 in the effluent.

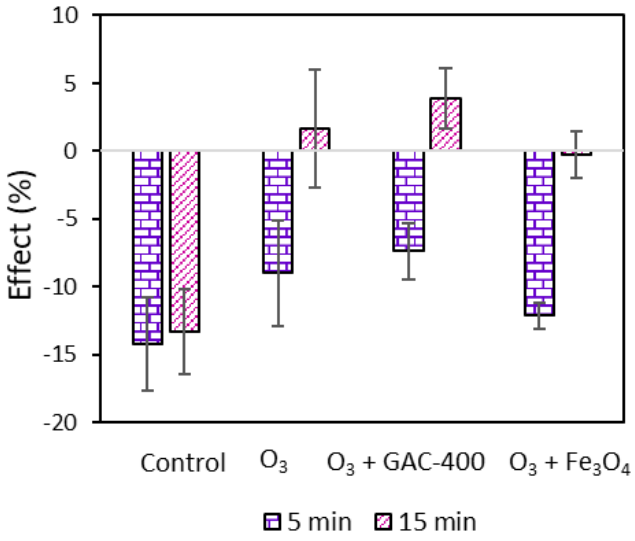

Figure 6. Inhibition of luminescence of *V. Fischeri* after 5 and 15 min of exposure to the effluents of MPs spiked CSO treated by single and catalytic ozonation with Fe_3O_4 and GAC-400. [O_3] =10 mg L^{-1}; [GAC-400 and Fe_3O_4] = 50 mg L^{-1}.

YES assay was also performed in this study. This test evaluates the potential estrogenic activity of treated water. The results are listed in Table 2.

Table 2. Percentage of Induction from YES assay for single and catalytic ozonation with Fe_3O_4, GAC-400. [O_3] = 10 mg L^{-1}; [GAC-400 and Fe_3O_4] = 50 mg L^{-1}.

Samples	**% Induction**
Control	2.3
Control	4.6
O_3	0.9
O_3	1.2
GAC-400	-0.4
GAC-400	0.8
Fe_3O_4	2.1
Fe_3O_4	2.1

Final effluents of single ozonation and catalytic ozonation with GAC-400 and Fe_3O_4 examined by YES assay presented percentages of induction below 10%, demonstrating no estrogenic activity for neither sample. Unlike Microtox assays, where the acute toxicity increased with the treatments, the % of induction decreases for estrogenic assays. Again, trial conducted with effluent obtained after H_2O_2-ozonation treatment killed all the yeast cell owing to the oxidizing nature of the residual H_2O_2. This fact evidences the necessity to evaluate the toxicity using different tests due to the different sensitivity of organisms.

Murine RAW 264.7 macrophage toxicity assay was carried out to identify the overall cytotoxic effects of treated CSO with single ozonation and catalytic ozonation with Fe_3O_4 and GAC-400. Different percentages of dilution of final effluents were evaluated: 10, 30, 50, 70 and 90% v/v and results were related to those obtained for the PBS dilution control (Fig. 7).

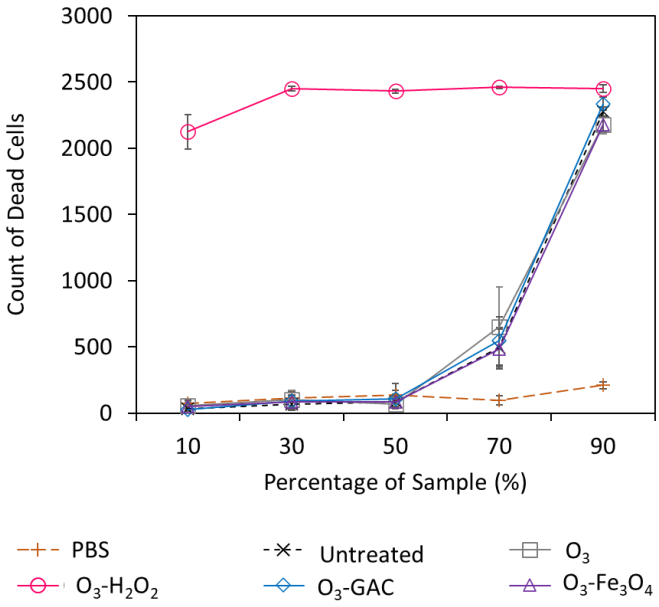

Figure 7. Cell line toxicity with 10, 30, 50, 70 and 90% of dilution of treatment for single and catalytic ozonation with Fe_3O_4, GAC-400 and H_2O_2. [O_3] =10 mg L^{-1}; [GAC-400 and Fe_3O_4] = 50 mg L^{-1}; ratio (H_2O_2/O_3) =0.25.

As can be observed in Fig. 7, PBS-exposed cells showed no significant changes in the number of dead cells at any dilution (i.e. % v/v) tested, indicating that changes in the volume of media up to 90% of a sample did not induce cytotoxic effects. For untreated

CSO and treated effluent with single ozonation and catalytic ozonation with Fe_3O_4 and GAC-400, the same trend among them was observed. When the percentage of sample was between 10 and 50% no changes in the number of dead cells was observed for GAC-400, Fe_3O_4 or single ozonation alone treated samples, indicating no cytotoxicity. However, for dilutions greater than 50% v/v, significant increases in the number of dead cells were observed for all CSO and treated effluent. For example, the number of dead cells ranged between 500 and 2200 at v/v/ dilutions of 70% and 90%, respectively. In comparison, H_2O_2 treated sample exposed cells showed significant increases in the number of dead cells at all dilutions examined relative to controls indicating significant cytotoxic effects. These profiles compared with untreated CSO indicate that treatments overall did not alter cytotoxicity of samples in anyway with the exception of the H_2O_2 treatment.

The cytotoxicity observed using the RAW 264.7 cell line was not fomented by MPs due to the reduction of these in different treatments. For untreated CSO with MPs at 50% of sample percentage, the percentage for all MPs was 50% and no cytotoxicity effect was observed. For other treatments (O_3, O_3+Fe_3O_4 and O_3+GAC-400) at 70 and 90% of sample, none of the MPs exceeded 50% of their concentration, indicating the effect is not caused by spiked MPs. These results can be found in supplementary material (Figure S2-S6).

Contrary to other treatments, catalytic ozonation with H_2O_2 presented high cytotoxicity with all percentages of sample. With a 10% v/v the number of dead cells was approximately 2000 and, at percentages from 30 to 90%, this number remained relatively high (~2300 cells). These results indicate that H_2O_2 treated water exposures are cytotoxic regardless of the dilution tested and this is likely due to non-consumed H_2O_2 within these treated samples with the maximum effect at a 30% v/v dilution.

The biodegradability is also an important assay to perform in the final treated effluent. The results are displayed in Table 3. As can be observed, the treatments performed with O_3, and catalytic ozonation with GAC-400 and Fe_3O_4, presented higher biodegradability than control. These results are a consequence of the MPs oxidation, leaving more simple structures which can be degraded by microorganisms. The highest biodegradability was shown with catalytic ozonation using GAC-400, which corresponds to the treatment with better results in MPs removal.

The lowest biodegradability was achieved in peroxone. However, the MPs removal was not the highest. Thus, probably the low value of DBO_5 was due to the inhibition of microorganisms by unreacted H_2O_2 as observed in the cell line test.

Table 3. Biodegradability for catalytic ozonation with Fe_3O_4, GAC-400 and H2O2. [O_3] = 10 mg L^{-1}; [GAC-400 and Fe3O4] = 50 mg L^{-1}; ratio mg H_2O_2/mg O_3 = 0.25

Samples	**mg L^{-1}**	**Standard Deviation**
Control	61.85	±8.55
O_3	66.20	±3.27
GAC-400	73.63	±0.22
Fe_3O_4	65.57	±8.99
H_2O_2	34.88	±7.23

4. Conclusions

Single and catalytic (using carbon, iron and peroxide based catalysts) ozonation has been studied for the remediation of MPs from CFS pretreated CSO. The CFS pretreatment significantly reduced the turbidity and DOC of the CSO but had minimal impact on UV_{254} and pH of the water. The prepared carbon based catalysts showed highest surface area and pore volumes compared to iron-based catalysts and their surfaces were either slight acidic (GAC, GAC-400 and SBC, prepared at low or medium temperatures) or basic (GAC-900 and GAC-U, prepared at high temperature with alkaline surface modification respectively). Among the carbon-based materials studied, SBC exhibited the highest adsorption capacity for the removal of MPs from the CFS pretreated CSO, even though it had lower surface area compared to GAC and its derivatives materials. Solid iron-based catalyst showed negligible adsorption capacity for the removal of the MPs.

In both single and catalytic ozonation, higher degradation efficiency of MPs was always observed at 10 mg L^{-1} O_3 dose compared to lower dose (5 mg L^{-1}) irrespective of the catalyst material used. The MPs degradation efficiency was enhanced by catalytic ozonation with optimum catalyst/peroxide dose except in the case of SBC. Additionally, the use of excess catalyst dosage resulted in declined degradation efficiency due to scavenging effect, catalyst aggregation (solid iron-based catalysts) or organic nature of the added oxidant (PAA).

Among the MPs, SMX (highly reactive) was easily and completely degraded even by single ozonation at lower O_3 dose. 2,4-D and MCP (medium reactivity) showed medium and excellent degradation efficiency at 5 and 10 mg L^{-1} O_3 dose, respectively, in both single and catalytic ozonation, except in the case of catalytic ozonation with SBC, where all the MPs were poorly removed from the CSO due to quenching of O_3 by the SBC catalyst. ATZ (highly resistant to oxidation by O_3) was least degraded among the MPs at all conditions studied.

GAC-400 showed the highest catalytic activity for the degradation of MPs during catalytic ozonation among the carbon-based catalysts. For iron-based catalysts, both ZVI and Fe_3O_4 showed similar and higher MPs degradation efficiency compared to Fe^{2+} at all conditions studied. Peroxone process showed better degradation of all the MPs compared to PAA-ozonation at all H_2O_2/O_3 ratio and O_3 doses.

The effluents obtained after single ozonation, catalytic ozonation using GAC-400 and Fe_3O_4 showed no significant acute toxicity to marine bacteria *V. fischeri*, estrogenicity towards yeast cells and cytotoxicity towards macrophage cell line. In contrast, effluent obtained after peroxone process exhibited high toxicity towards all the microorganisms studied, due to the strong oxidation nature of the residual H_2O_2. Both single ozonation and catalytic ozonation using GAC-400 and Fe_3O_4 treatments improved the biodegradability of the organics in spiked CSO, but peroxone treatment did not.

The combined CFS and ozonation processes can be an effective treatment strategy for the remediation of MPs from sewer overflow prior to discharge to the environment.

Acknowledgments

The authors acknowledge the financial support provided by a research grant from Natural Sciences and Engineering Research Council of Canada (NSERC) Collaborative Research and Development (CRD) program, Spanish Ministry of Education, Culture and Sports (FPU research fellowship FPU-16/02101 and FPU short stay fellowship EST17/00566 of Núria López) and Spanish Ministry of Economy and Competitiveness (FPI research fellowship BES-2015-074109 of Alberto Cruz).

References

Acero, J.L., Stemmler, K., von Gunten, U., Degradation kinetics of atrazine and its degradation products with ozone and ·OH radicals: A predictive tool for drinking water treatment, Environ. Sci. Technol. 34 (2000) 591–597.

Alameddine, M., Al Umairi A., Shaikh, M.Z., Gamal El-Din, M., Bench to Full-Scale Enhanced Primary Treatment of Municipal Wastewater under Wet Weather Flow for Minimized Pollution Load: Evaluation of Chemical Addition and Process Control Indicators, Can. J. Civ. Eng. (2020), doi.org/10.1139/cjce-2019-0515.

Bader, H., Hoigné, J., Determination of ozone in water by the indigo method. Water Res. 15 (1981) 449–456.

Beltrán, F.J., González, M., Rivas, J., Marin, M., Oxidation of mecoprop in water with ozone and ozone combined with hydrogen peroxide, Ind. & Eng. Chem. Res. 33 (1994) 125-136.

Beltran, F.J., Rivas, F.J., Montero-de-Espinosa, R., Iron type catalysts for the ozonation of oxalic acid in water, Water Res. 39 (2005) 3553–3564.

Benitez, F.J., Acero, J.L., Real, F.J., Roman, S., Oxidation of MCPA and 2,4-D by UV radiation, ozone, and the combinations UV/H_2O_2 and O_3/H_2O_2, J. Enviro. Sci. health, Part B: Pesticides, Food Contaminants, and Agricultural Wastes 39 (2004) 393–409.

Blackbeard, J., Lloyd, J., Magyar, M., Mieog, J., Linden, K.G, Lester, Y., Demonstrating organic contaminant removal in an ozone-based water reuse process ar full scale, Environ. Sci. Water Res. Technol., 2 (2016) 213-222.

Bourgin, M., Beck, B., Boehler, M., Borowska, E., Fleiner, J., Salhi, E., Teichler, R., von Gunten, U., Siegrist, H., McArdell, C.S., Evaluation of a full-scale wastewater treatment plant upgraded with ozonation and biological post-treatments: abatement of micropollutants, formation of transformation products and oxidation byproducts, Water Res. 129 (2018) 486–498.

Brillas, E., Sirés, I., Oturan, M.A., Electro-Fenton process and related electrochemical technologies based on Fenton's reaction chemistry, Chem. Rev. 109 (2009) 6570–6631.

Cruz-Alcalde, A., Esplugas, S., Sans, C., Abatement of ozone-recalcitrant micropollutants during municipal wastewater ozonation: Kinetic modelling and surrogate-based control strategies, Chem. Eng. J. 360 (2019a) 1092–1100.

Cruz-Alcalde, A., Esplugas, S., Sans, C., Continuous versus single H_2O_2 addition in peroxone process: performance improvement and modelling in wastewater effluents, J of Hazard. Mater. 387 (2019b) 121993.

De la Cruz, N., Giménez, J., Esplugas. S., Grandjean, D., de Alencastro, L.F., Pulgarin, C., Degradation of 32 emergent contaminants by UV and neutral photo-Fenton in domestic wastewater effluent previously treated by activated sludge, Water Res. 46 (2012) 1947–1957.

Dogruel, S., Cetinkaya Atesci, Z., Aydin, E., Pehlivanoglu-Mantas, E., Ozonation in advanced treatment of secondary municipal wastewater effluents for the removal of micropollutants, Environ. Sci. Pollut. Res. 27 (2020) 45460-45475.

El Samrani, A. G., Lartiges, B. S., Villiéras, F., Chemical coagulation of combined sewer overflow: Heavy metal removal and treatment optimization, Water Res. 42 (2008) 951–960.

Figueiredo, J.L., Pereira, M.F.R., Freitas, M.M.A., Órfão, J.J.M., Modification of the surface chemistry of activated carbons, Carbon 37 (1999) 1379–1389.

Ganiyu, S.O., Zhou, M., Martinez-Huitle, C.A., Heterogeneous electro-Fenton and photoelectro-Fenton processes: a critical review of fundamental principles and application for water/wastewater treatment, Applied Cat. B: Environ. 235 (2018) 103–129.

Ganiyu, S.O., van Hullebusch, Cretin, M., Esposito, G., Oturan, M.A., Coupling of membrane filtration and advanced oxidation processes for removal of pharmaceutical residues: A critical review, Sep. & Purif. Technol. 156 (2015) 891–914.

Gonçalves, A.G., Órfão, J.J.M., Pereira, M.F.R., Catalytic ozonation of sulfamethoxazole in the presence of carbon materials: Catalytic performance and reactions pathways, J Hazard. Mater. 239–240 (2012) 167–174.

Huber, M.M., Canonica, S., Park, G.Y., Von Gunten, U., Oxidation of pharmaceuticals during ozonation and advanced oxidation processes, Environ. Sci. Technol. 37 (2003) 1016–1024.

Kumar Chhetri, R., Thornberg, D., Berner, J., Gramstad, R., Öjstedt, U., Kumari Sharme, A., Rasmus Andersen, H., Chemical disinfection of combined Sewer Overflow waters using performic acid or peracetic acids, Sci. Total Environ. 490 (2014) 1065-1072.

Kumar Chhetri, R., Bonnerup, A., Rasmus Andersen, H., Combined Sewer Overflow pretreatment with chemical coagulation and a particle settler for improved peracetic acid disinfection, J. Ind. Eng. Chem. 37 (2016) 372-379.

Lee, Y., Gerrity, D., Lee, M., Encinas Bogeat, A. Salhi, E., Gamage, S., Trenholm, R.A., Wert, E.C., Snyder, S.A., von Gunten, U., Prediction of micropollutant elimination during ozonation of municipal wastewater effluents: use of kinetic and water specific information, Environ. Sci. & Technol. 47 (2013) 5872–5881.

Lee, Y., von Gunten, U., Oxidative transformation of micropollutants during municipal wastewater treatment: comparison of kinetic aspects of selective (chlorine, chlorine dioxide, ferrate VI, and ozone) and non-selective oxidants (hydroxyl radical). Water Res. 44 (2009) 555–66.

Li, X., Chen, W., Ma, L., Wang, H., Fan, J., Industrial wastewater advanced treatment via catalytic ozonation with an Fe-based catalyst, Chemosphere 195 (2018) 336–343.

López-Vinent, N., Cruz-Alcalde, A., Gutiérrez, C., Marco, P., Giménez, J., Esplugas, S., Micropollutant removal in real WW by photo-Fenton (circumneutral and acid pH) with BLB and LED lamps, Chem. Eng. J. 379 (2020)122416.

López-Vinent, N., Cruz-Alcalde, A., Romero, L.E., Chávez, M.E., Marco, P., Giménez, J., Esplugas, S., Synergies, radiation and kinetics in photo-Fenton process with UVA-LEDs, J Hazard. Mater. 380 (2019) 120882.

López, N., Plaza, S., Afkhami, A., Marco, P., Giménez, J., Esplugas, S., Treatment of Diphenydramine with different AOPs including photo-Fenton at circumneutral pH, Chem. Eng. J. 318 (2017) 112–120.

Luukkonen, T., Pehkonen, S.O., Peracids in water treatment: A critical review, Crit. Rev. of Environ. Sci. Technol. 47 (2017) 1−39.

Malvestiti, J.A., A. Cruz-Alcalde, N. López-Vinent, R. F. Dantas, C. Sans, Catalytic ozonation by metal ions for municipal wastewater disinfection and simulataneous micropollutants removal, Appl. Catal. B: Environ 259 (2019) 118104.

Mecha, A.C., Onyango, M.S., Ochieng, A., Momba., M.N.B., Impact of ozonation in removing organic micropollutants in primary and secondary municipal wastewater: effect of process parameters. Water Sci. Technol. 74 (3) (2016) 756-765.

Meiquan, C., P. Sun, L. Zhang, C-H, Huang, UV/Peracetic acid for degradation of pharmaceuticals and reactive species evaluation, Environ. Sci. & Technol. 51 (2017) 14217-14224.

Ortiz de García, S., Pinto Pinto, G., García Encina, P., Irusta Mata, R., Consumption and occurrence of pharmaceutical and personal care products in the aquatic environment in Spain, Sci. Total Environ 444 (2013) 451-465.

Rajah, Z., Guiza, M., Solís, R.R., Rivas, F.J., Ouederni, A., Catalytic and photocatalytic ozonation with activated carbon as technologies in the removal of aqueous micropollutants, J. Photochem. Photobiol. A. 382 (2019) 111961.

Richardson, S. D. and Kimura, S. Y., Water Analysis: Emerging contaminants and current issues, Anal. Chem. 88,1 (2016) 546-582.

Riechel, M., Matzinger, A., Pallasch, M., Joswig, K., Pawlowsky-Reusing, E., Hinkelmann, R., Rouault, P., Sustainable urban drainage systems in established city developments: Modelling the potential for CSO reduction and river impact mitigation, J. Environ. Manage. 274 (2020) 111207.

Sanchez-Polo, M., von Gunten, U., Rivera-Utrill, J., Efficiency of activated carbon to transform ozone into $^{\bullet}OH$ radicals: Influence of operational parameters, Water Res. 39 (2005) 3189–3198.

867 Singh, S., Seth, R., Tabe, S., Yang, P., Oxidation of emerging contaminants during pilot-
868 scale ozonation of secondary treated municipal effluent, ozone Sci. Eng. 37 (4) (2015)
869 323-329.

870 Tondera, K., Klaer, K., Gebhardt, J., Wingender, J., Koch, C., Horstkott, M., Strathmann,
871 M., Jurzik, L., Hamza, I.A., Pinnekamp, J., Reducing pathogens in combined sewer
872 overflows using ozonation or UV irradiation, Int. J. Hyg. Environ. Health218 (2015)
873 731–741

874 Vatankhah, H., Riley, S.M., Murray, C., Quinones, O., Xerxes Steirer, K., Dickenson,
875 E.R.V., Bellona, C., Simultaneous ozone and granular activated carbon for advanced
876 treatment of micropollutants in municipal wastewater effluent, Chemosphere 234
877 (2019) 845-854.

878 von Gunten. U., Ozonation of drinking water: Part II. Disinfection and by-product
879 formation in presence of bromide, iodide or chlorine. Water Res. 37 (2003) 1469–
880 1487.

881 Wojtenko, I., Performance of ozone as a disinfectant for combined sewer overflow. Crit.
882 l Rev. Environ. Sci. Technol. 31 (2001) 295–309.

883 Yin, R., Guo, W., Zhou, X., Zheng, H., Du, J., Wu, Q., Chang, J., Ren, N., Enhanced
884 sulfamethoxazole ozonation by noble metal-free catalysis based on magnetic Fe_3O_4
885 nanoparticles : catalytic performance and degradation mechanism, RSC Adv. 6 (2016)
886 19265

887 Zhu, H., Ma, W., Han, H., Han, Y., Ma. W., Catalytic ozonation of quinoline using nano-
888 MgO: Efficacy, pathways, mechanisms and its application to real biologically
889 pretreated coal gasification wastewater, Chem. Eng. J 327 (2017) 91–99.

890 Ziylan, A., Ince, N.H., Catalytic ozonation of ibuprofen with ultrasound and Fe-based
891 catalysts, Cat. Today 240 (2015) 2–8.

Supplementary Information for

Coagulation-flocculation followed by catalytic ozonation processes for enhanced primary treatment during wet weather conditions

Núria López-Vinent[1], Alberto Cruz-Alcalde[1], Soliu O. Ganiyu[2], Shailesh Sable[2], Selamawit Ashagre Messele[2], Dustin Lillico[3], James Stafford[3], Carmen Sans[1], Jaime Giménez[1], Santiago Esplugas[1*], Mohamed Gamal El-Din[2*]

[1]*Department of Chemical Engineering and Analytical Chemistry, Faculty of Chemistry, University of Barcelona, C/Martí i Franqués 1, 08028 - Barcelona, Spain. Tel: +34934020154. Fax: +34934021291*

[2]*Department of Civil and Environmental Engineering, Faculty of Engineering, University of Alberta, 9211-116 Street NW, T6G 1H9 - Edmonton, Canada. Tel: 1-780-492-5124*

[3]*Department of Biological Sciences, 11355 - Saskatchewan Drive, University of Alberta, Edmonton, Alberta T6G 2E9, Canada. Tel: 1-780-492-9258*

*Corresponding Authors: Santiago Esplugas (e-mail: santi.esplugas@ub.edu) and Mohamed Gamal El-Din (mgamalel-din@ualberta.ca)

Table of Contents

Text S1. Preparation of the carbon-based catalysts

Untreated GAC was the starting material to prepare three surfaced modified GACs (GAC-400, GAC-900 and GAC-U). Table 1 shows a brief catalyst description and their corresponding abbreviations. The methods used to prepare these materials were described elsewhere [Messele et al., 2015; Messele et al., 2014; Pereira et al., 2003]. The starting GAC was first oxidized with nitric acid (HNO_3, 6M) and then heat-treated under a flow of N_2 at 400 ^oC (GAC-400) and 900 ^oC (GAC-900), respectively. For GAC-U, the starting material was impregnated with urea and heat-treated at 400 ^oC, under a flow of N_2. A sludge-based catalyst (SBC) is also included in Table 1 and it was prepared by a method previously reported [Li et al., 2016]. Commercial Fe_3O_4 (Nanostructured & Amorphous Materials, Inc. USA; particle size: 50-100 nm and purity: 97%) and ZVI (Connelly – GMP, Inc. USA; particle size: 40-60 nm; purity: 99%) were also used as solid catalysts in this study.

Table S1. Description and notation of prepared carbon-based catalysts

Abbreviation	Catalyst description
SBC	Dried sludge modified with $ZnCl_2$ and carbonized at 600 ^oC
GAC-400	HNO_3-treated GAC, and heat-treated under N_2 flow at 400 ^oC
GAC-900	HNO_3-treated GAC, and heat-treated under N_2 flow at 900 ^oC
GAC-U	Urea-treated GAC, and heat-treated under N_2 flow at 400 ^oC

Text S2. Characterization of the catalysts

N_2 adsorption measurements were performed at –196 ^oC on gas adsorption system ASAP 2000 (Micrometrics, USA). Prior to the measurements, the catalyst sample was grounded to particle size of $\leq 2\mu m$ and about 100 mg was outgassed at 120 ^oC for 5 h under vacuum. The specific surface area of the mesopores (S_{meso}) and the micropore volume (V_{micro}) were calculated by the t-method [de Boer et al., 1966]. Moreover, the surface area (S_{BET}) and the pore size of the sample was calculated by the Brunauer–Emmett–Teller (BET) method [Brunauer et al., 1932] and Barrett-Joyner-Halenda (BJH) method [Barrett et al., 1951], respectively. Point of zero charge (pHpzc) of the carbon-based materials was determined using a solid addition method. 50 mL aliquots of 0.1 M NaCl solutions were adjusted to initial pH (pH_0) between 3 and 12 using 0.1 M HCl or NaOH and transferred to 125 mL

stoppered flasks. 1 g of each grounded carbon sample (≤ 2μm) was added to the stoppered flasks, and capped immediately. Suspensions were shaken for 48 h to allow them to reach equilibrium and the final pH (pH_f) of the supernatant was recorded. The difference between the final and initial pH values ($\Delta pH = pH_f - pH_0$) was plotted against the pH_0. The point of intersection of the curve at which $\Delta pH = 0$ corresponds to the pH_{PZC}. Surface morphology and elemental composition of the prepared carbon-based catalysts was recorded on scanning electron microscope (SEM-EDX, VEGA 3 Tescan, Tescan USA, Inc., PA, USA). The samples were fixed with 2.5% (v/v) glutaraldehyde ($C_5H_8O_2$) and 1.0% (v/v) osmium tetroxide (OsO_4) (Ted Pella Inc., Redding, CA, USA) in phosphate buffered saline (PBS) for 24 h. After fixation, the samples were dehydrated with 50, 70, and 100% ethanol (C_2H_5OH) and dried completely in a critical point dryer. Carbon material samples were attached to an aluminum sample holder with carbon tape and sputter coated with gold for 30 s prior to imaging.

Text S3. Toxicity tests

The acute toxicity of the solution was assessed via *Vibrio fischeri* bioluminescence inhibition assay using Microtox® standard method (Azur Environmental, Delaware USA). All samples were check (and adjusted if necessary) to ensure it is around circum-neutral (6.5 – 7.5) pH values and 100 μL of osmotic adjustment solution (22% NaCl solution) was added to 900 μL sample to ensure an osmotic protection for bacteria. The bioluminescence inhibition percentage was measured after 5 and 15 min using the M500 microplate reader equipment (BioTek Instruments, USA).

The estrogenicity of the samples was assessed using yeast assay test using β-galactosidase and estrogen (YES) cell following the procedure described in ISO/DIS 19040-2 [Hettwer et al., 2018]. Hettwer and coworkers have reported the details of this method [Hettwer et al., 2018]. Briefly, 10 μL of dimethysulfoxide was added to 990 μL of the sample in well plate and kept at 4 ^oC prior to analysis. Freeze-dried yeast cells were washed three times with alternating centrifugation and resuspension steps. The washed cell was reactivated at 30 ^oC for 1 h on an incubation shaker. 100 μL of YES cells are diluted with 900 μL growth medium. To all the needed well plate, 300 μL of the dilute YES was added to the samples. The plate was sealed with gas permeable foil and incubated at 31 ^oC during 18 h with agitation (100 rpm). After incubation, the assay was read at 690 nm and the data used to calculate growth factor. New well plate was filled with 50 μL of sample, thoroughly mixed and 30 μL of incubated dilute YES was added. The mixture was

incubated for 30 min at 31 ^{o}C with agitation (100 rpm). The OD_{570} and OD_{590} of each plate was read on plate reader.

Text S4. Biodegradability

The biodegradability of the untreated and treated MPs spiked CSO samples was assessed using biological oxygen demands after five days (BOD_5). An YSI^{TM} Pro 20 DO kits (YSI^{TM}, USA) was used to measure the initial and final dissolved oxygen (DO) for both treated and untreated MPs spiked CSO. The phosphate buffer solution was prepared by dissolving 42.5 g of potassium phosphate monobasic (KH_2PO_4) and 1.7 g of ammonium chloride (NH_4Cl) in 1 L Milli-Q water and the pH adjusted to 7.3 with 30% sodium hydroxide (NaOH). Solutions of magnesium sulfate ($MgSO_4$) (22.5 g L^{-1}), iron III chloride ($FeCl_3$) (0.22 g L^{-1}) and calcium chloride ($CaCl_2$) (27.5 g L^{-1}) were prepared using the analytical grade of the chemicals. In all samples, pH was checked to ensure it was between 7.0 – 7.5. Dilution water used for the biodegradability test was prepared by transferring 10 L deionized water into tank and aerated for 12 h to enhance the DO concentration. 1 mL each of prepared phosphate buffer, $MgSO_4$, $CaCl_2$ and $FeCl_3$ solution was added per liter of dilution water and mixed thoroughly to ensure homogenization. A 300 mL BOD bottle was used for all the tests. Each bottle contained 10 mL sample, 2.5 mL seed suspension (prepared from raw activated sludge obtained from municipal wastewater treatment plant) and the rest was filled with dilution water. Seed, water and glucose-glutamic acid check samples were prepared to evaluate the activity of the microbial community. All the samples were incubated for 5 days at temperature of 20 ^{0}C. The BOD_5 was estimated from Eq. (1):

$$BOD_5, (mg\ L^{-1}) = \frac{(D_1 - D_2) - (S)V_s}{p} \quad (1)$$

where D_1 and D_2 are the *DO* of diluted sample immediately after preparation and after 5 days incubation (mg L^{-1}), *S* is oxygen uptake of seed, *Vs* is volume of seed in the test bottle (mL) and *p* is the decimal volumetric fraction of sample used.

Text S5. Mouse Macrophage Cell Viability Assay

The *in-vitro* viability of mouse immune cells exposed to various water samples (untreated vs treated) was examined as a measure of their immunocytotoxic effects. Specifically, RAW 264.7 mouse macrophage cells were seeded (5×10^5 cells per well) into a 24-well culture plate and incubated at 37 °C/5% CO_2 overnight in complete cell culture media (Dulbecco's Modified Eagle Medium (DMEM); Sigma, Canada). The following day, cells were exposed to water samples at dilution doses between 10-90% v/v, for 18 h at 37 °C. To control for any changes in viability due to media displacement, cells were also exposed to phosphate buffered saline solution (PBS; Sigma Canada) at all dilutions tested for the experimental waters (i.e. 10-90% v/v). After 18 h, cell viability was examined by first detaching cells from culture wells using 1 mM ethylenediaminetetraacetic acid (EDTA) in 0.25% trypsin (Sigma, Canada) and transferring them to 1.5 mL centrifuge tubes. Cells were then stained for the absence or presence of free amines, a marker of cell death, on both the plasma membrane as well as intracellularly by incubating cells with PBS containing 0.1% v/v of the cell permeable Live-Dead Yellow Cell Stain (Thermofisher, Canada) for 30 min at room temperature. By staining for increased membrane and intracellular free amines, cells that are alive (i.e. no significant free amines present) and those cells that are dead (i.e. significant free amines present) can be distinguished using flow cytometric analysis. After live/dead staining was performed, cells were washed twice with 500 µL of PBS to remove any excess staining solution and were then re-suspended in 1% paraformaldehyde (PFA; Sigma, Canada) for 30 min at 4 °C for cell fixation. Cells were then examined using an Imagestream^{TM} Mark II (Amnis Corporation) for the absence or presence of the live/dead stain. Three independent experiments were conducted for each water sample exposure and data represents the mean of these experiments ±SEM. Statistics were conducted using a two-tailed paired Student T-test with a significance of $P<0.05$.

Text S6. Textural properties of solid catalysts

Textural properties, such as specific surface area (S_{BET}, $m^2\ g^{-1}$), total pore volume (V_{total}, $cm^3\ g^{-1}$) and micropore or mesopore nature (S_{micro} and S_{meso}, $m^2\ g^{-1}$, and V_{micro} and V_{meso}, $cm^3\ g^{-1}$) of carbon and iron-based catalysts are shown in Table S2. The pH_{pzc} values have been also included. All carbon-based catalysts had a large S_{BET}. The highest S_{BET} was

obtained for the GAC-900 (1002 m^2 g^{-1}) and the smallest was for SBC (583 m^2 g^{-1}). The materials derivatives of GAC had also high S_{BET} and are essentially microporous (S_{micro} > S_{meso}). However, SBC presented results in the same order of magnitude for specific mesopore surface area and specific micropore surface area, representing a significant difference compared to GAC-based materials. In fact, contrary to GAC derivatives, SBC had higher mesoporous (331 m^2 g^{-1}) than microporous (252 m^2 g^{-1}) specific surface. These differences in carbon materials were also reflected by the ratio V_{micro}/V_{total}. In particular, SBC had a ratio V_{micro}/V_{total} = 0.16, while GAC derivatives revealed an intermediate microporous character with V_{micro}/V_{total} = 0.64, 0.65, 0.62 and 0.57 for GAC, GAC-400, GAC-900 and GAC-U, respectively.

The thermal treatment at 900 ºC enabled the development of further porosity in GAC-900 (S_{BET} GAC-900 > S_{BET} GAC). However, when lower temperature was applied to the catalyst (GAC-400) a lower porosity was detected. Although differences in the porosity were observed between the catalysts prepared by thermal treatment, and HNO_3 and GAC, these were minimal. The highest differences concerning the porosity and V_{micro}/V_{total} ratio were observed between GAC and GAC-U.

The values of pH_{pzc} are important to know the acidic or basic nature of the adsorbent, which is related to functional groups. Thus, the pH_{pzc} evaluation is important for the determination of the predominant functional groups present in the material, and their influence on MPs adsorption/degradation. The acidic functional groups include carboxylic acids, lactones and phenols. The basic functional groups are carbonyls and quinones, pyrenes and chromenes [Figueiredo et al., 2007]. As can be observed in Table 3, the surface nature of all carbon-based catalysts is near neutral, indicating the presence of both basic and acidic functional group. These functional groups have been reported to be crucial in activation of oxidant precursors such as persulfate and subsequent MPs degradation [Cheng et al., 2017]. GAC-900 shown the highest value of pH_{pzc} (8.1) and GAC-400 presented the lowest (5.9). The starting material, GAC, shown a value of pH_{pzc} of 6.2 being similar than GAC-400. The low temperature applied to the treatment (400 ºC) was not enough to remove the acidic functional groups, and the employment of HNO_3 could have lowered a little the pH_{pzc} value [Messele et al., 2015]. The high temperature (900 ºC) used to produce GAC-900 removed the most acidic groups, leaving in the surface functional groups with a more basic nature [Pereira et al., 2003]. In the case of GAC-U, even though the temperature of the treatment (400 ºC) was low, the introduction of urea

seems to be enough to change the nature of the starting material increasing the basicity of its surface [Messele et al., 2014].

Table S2. Textural properties of the carbon-based and iron-based catalysts

Catalyst	S_{BET} ($m^2\ g^{-1}$)[1]	S_{micro} ($m^2\ g^{-1}$)[2]	S_{meso} ($m^2\ g^{-1}$)[3]	V_{total} ($cm^3\ g^{-1}$)[4]	V_{micro} ($cm^3\ g^{-1}$)[5]	V_{meso} ($cm^3\ g^{-1}$)[6]	pH_{pzc}[7]
SBC	583	252	331	0.740	0.115	0.625	6.9
GAC	976	839	137	0.599	0.386	0.213	6.2
GAC-400	959	832	127	0.549	0.358	0.191	5.9
GAC-900	1002	861	141	0.582	0.363	0.219	8.1
GAC-U	883	770	113	0.487	0.278	0.209	7.5
Fe_3O_4	326.0	145.0	181.0	0.128	0.087	0.215	n.a
ZVI	121.0	49.0	72.0	0.112	0.086	0.198	n.a

[1] S_{BET} is the BET-specific surface area
[2] S_{micro} is the *t*-plot-specific micropore surface area calculated from the N_2 adsorption-desorption isotherm
[3] S_{meso} is the specific mesopore surface area estimated by subtracting Smicro from SBET
[4] V_{total} is the total specific pore volume determined by using the adsorption branch of the N_2 isotherm at P/P_0=0.99
[5] V_{micro} is the specific micropore volume calculated by a non-local density functional theory (NLDFT) method
[6] V_{meso} is the specific mesopore volume calculated by subtracting V_{micro} from V_{total}
[7] pH_{pzc} is the pH at the point of zero charge

Text S7. Elemental composition and morphology of solid catalysts

The elemental compositions of the carbon-based and iron-based materials are shown in Table S3. The acidic nature of the GAC-400 could be due to the introduction of carboxylic groups in the course of the treatment, in accordance with the oxygen content and the value of pH_{pzc}, compared to commercial GAC [Álvarez-Torrellas et al., 2016]. However, in the case of GAC-900 the small increase in the oxygen percentage (7.34 wt% for GAC and 8.35 wt% for GAC-900) did not involve an increase in the acidic character, in accordance with the value of pH_{pzc}. This is probably explained by a higher amount of oxygen functionalities such as carbonyl, chromenes and pyrenes compared to other more acidic groups. The highest value of oxygen content corresponded to SBC (20.35%), being thus the most hydrophilic material [Álvarez-Torrellas et al., 2016]. Regarding nitrogen content, GAC-U, doped with urea, was the material with high percentage of this element (3.50 wt%). The other carbon-based catalysts shown small percentage of nitrogen (from 0.08 wt% to 0.85 wt%).

SEM images of carbon-based materials were acquired to study the morphological characteristics of each carbon-based material. These are shown in Fig. S1. Morphology

of the SBC (Fig. S1a) shows different surface than other GAC derivatives materials (Fig. S1b–e). For example, the presence of mesoporous is more remarkable in SBC than that in other catalysts, which agrees with the N_2 adsorption analysis. Fig. S1b–d, on the contrary, present similar morphology with more micropores and less dense structure compared to SBC. Nevertheless, Fig. S1e, corresponding to GAC-U is not so similar than the other GAC derivatives materials, probably due to the treatment with urea and subsequent incorporation of more nitrogen content.

The FTIR spectra for the carbon based materials are shown in Fig. S1f. Two distinct absorption bands was observed in all the carbon-based materials; however, the spectra of the SBC exhibited more intense peaks compared to other carbon materials. This implies that the density of the functional groups on the SBC is higher which was expected because of the raw materials and temperature used to synthesize it. The band at 1620 cm^{-1} could be attributed to the vibration of C=C and C=O in the structure of the aromatic carbon, while the band at 1110 cm^{-1} can be assigned to C–O–H of the aliphatic groups of the SBC [Messele et al., 2014]. Other bands at the lower wavelength (745 – 873 cm^{-1}) in the spectra of the SBC maybe ascribed to vibration band of metallic oxides such as Zn, Fe and Si [Messele et al., 2015]. This agrees with the compositional analysis of the carbon-based materials which showed that the SBC contains significant amounts of Zn, Fe, and Si.

Table S3. Elemental analysis of the carbon-based and iron-based catalysts

Catalyst	C (wt%)	O (wt%)	N (wt%)	Na (wt%)	Al (wt%)	Si (wt%)	P (wt%)	S (wt%)	K (wt%)	Ti (wt%)	Fe (wt%)	Zn (wt%)
SBC	63.77	20.35	0.08	0.24	0.90	6.94	0.08	0.61	0.14	0.32	2.89	3.68
GAC	90.02	7.34	0.12	n.a	0.85	0.70	n.a	0.56	n.a	n.a	0.75	n.a
GAC-400	86.82	11.21	0.19	n.a	0.72	0.75	n.a	0.65	n.a	n.a	0.59	n.a
GAC-900	89.08	8.35	0.09	n.a	0.81	0.68	n.a	0.69	n.a	n.a	0.62	n.a
GAC-U	85.30	10.93	3.50	n.a	0.76	0.63	n.a	0.58	n.a	n.a	0.52	n.a
Fe_3O_4	-	32.15	-	-	-	-	-	-	-	-	67.8	-
ZVI	-	-	-	0.03	-	-	-	-	-	-	99.97	-

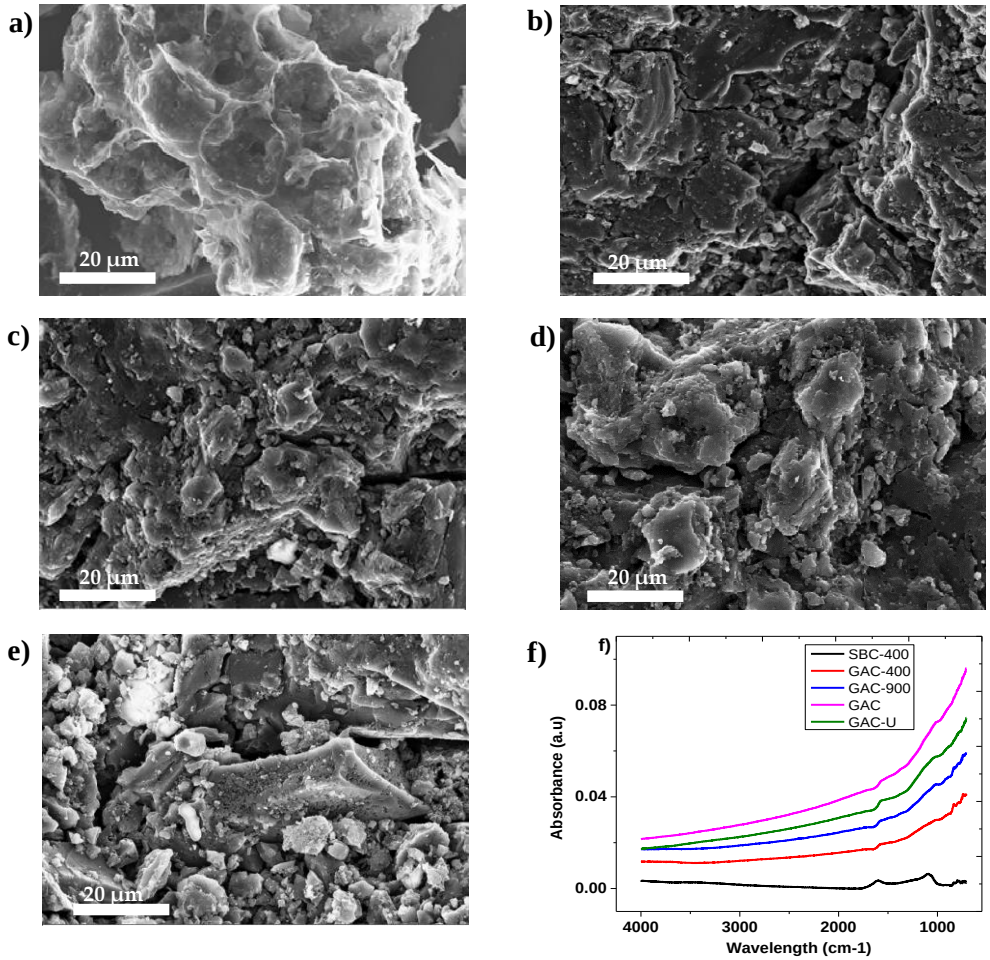

Figure S1. SEM images of a) SBC, b) GAC, c) GAC-400, d) GAC-900 and e) GAC-U and f) FTIR of (a – e).

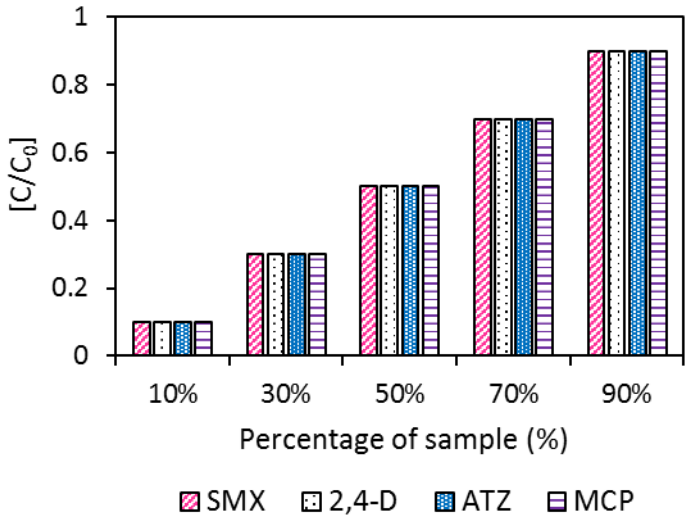

Figure S2. Concentrations of ATZ, SMX, 2,4-D and MCP for different dilutions of the sample in untreated CSO containing 1 mg L^{-1} each of the MPs (pH of the solution is 7.5).

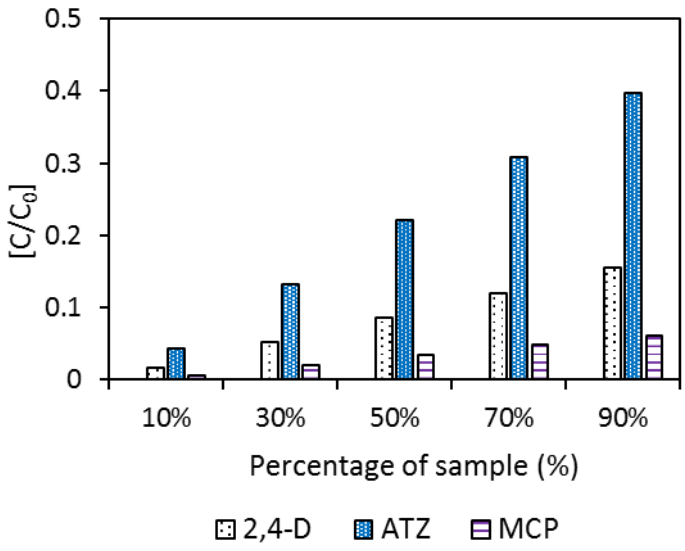

Figure S3. Concentrations of ATZ, 2,4-D and MCP for different dilutions of the sample in single ozonation containing 1 mg L^{-1} each of the MPs (pH of the solution is 7.5); [O_3]= 10 mg L^{-1}.

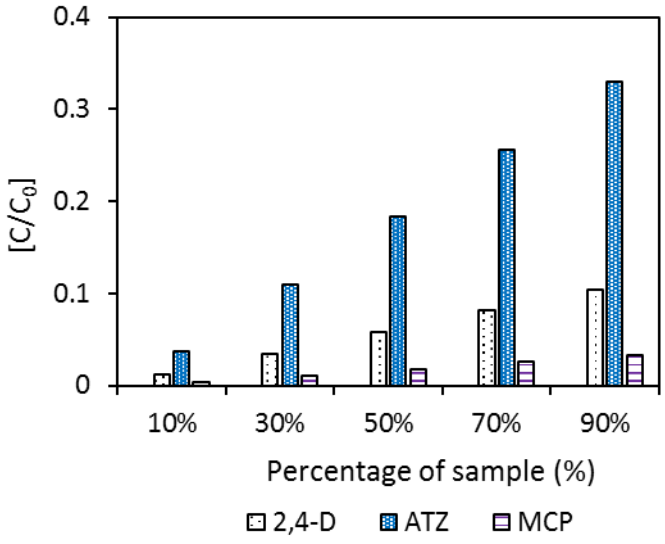

Figure S4. Concentrations of ATZ, 2,4-D and MCP for different dilutions of the sample in catalytic ozonation with Fe_3O_4 containing 1 mg L^{-1} each of the MPs (pH of the solution is 7.5); [O_3]= 10 mg L^{-1}; [Fe_3O_4]= 50 mg L^{-1}.

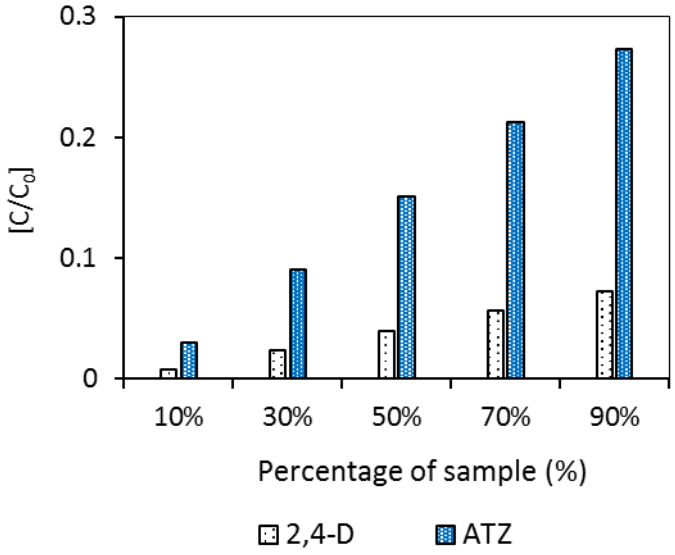

Figure S5. Concentrations of ATZ, and 2,4-D for different dilutions of the sample in catalytic ozonation with GAC-400 containing 1 mg L^{-1} each of the MPs (pH of the solution is 7.5); [O_3]= 10 mg L^{-1}; [GAC-400]= 50 mg L^{-1}.

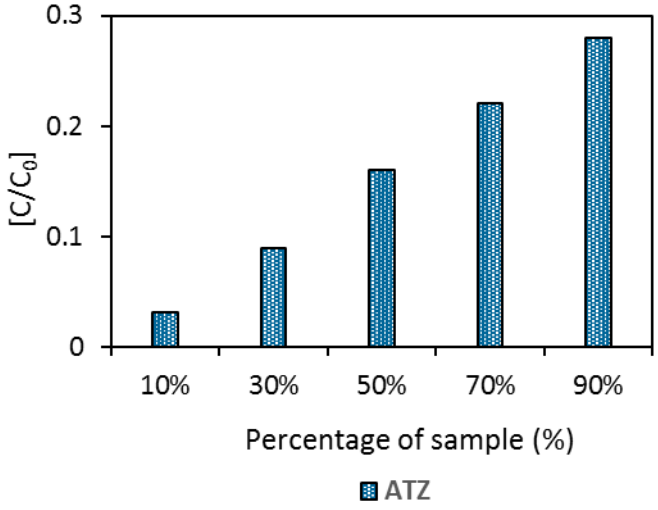

Figure S6. Concentration of ATZ for different dilutions of the sample in catalytic ozonation with H_2O_2 containing 1 mg L^{-1} of ATZ (pH of the solution is 7.5); [O_3]= 10 mg L^{-1}; ratio (H_2O_2/O_3) =0.25.

References

Álvarez-Torrellas, S., Ribeiro, R.S., Gomes, H.T., Ovejero, G., García, J., Removal of antibiotic compounds by adsorption using glycerol-based carbon materials, Chem. Eng. J. (2016) 296, 277–288.

Barrett, E.P., Joyner, L.G., Halenda, P.P., The determination of pore volume and area distributions in porous substances. I. Computations from nitrogen isotherms. J. Amer. Chem. Soc. 73 (1951) 373–380.

Brunauer, S., Emmett, P.H., Teller, E., Adsorption of gases in multimolecular layers. J. Am. Chem. Soc. 60 (1983) 09–319.

De Boer, J.H., Lippens, B.C., Linsen, B.G., The t-curve of multimolecular N_2-adsorption. J. Colloid Interface Sci. 21 (1966) 405–414.

Cheng, X., Guo, H., Zhang, Y., Wu, X., Non-photochemical production of singlet oxygen via activation of persulfate by carbon nanotubes, Water Res. 113 (2017) 80–88.

Figueiredo, J.L., Pereira, M.F.R., Freitas, M.M.A., Órfão, J.J.M., Characterization of active sites on carbon catalysts, Ind. & Eng. Chem. Res. 46 (2007) 4110–4115.

Hettwer, K., Jähne, M., Frost, K., Giersberg, M., Kunze, G., Trimborn, M., Reif, M., Türk, J., Gehramnn, L., Dardenne, F., De Croock, F., Abraham, M., Schoop, A., Waniek, J.J., Bucher, T., Simon, E., Vermeirssen, E., Werner, A., Hellauer, K., Wallentits, U., Drewes, J.E., Dietzmann, D., Routledge, E., Beresford, N., Zietek, T., Siebler, M., Simon, A., Bielak, H., Hollert, H., Müller, Y., Harff, M., Schiwy, S., Simon, K., Uhling, S., 2018. Validation of *Arxula* Yeast Estrogen Screen assay for detection of estrogenic activity in water samples: Results of an international interlaboratory study Sci. tot. Environ. 621, 612–625.

Li, Y., Li, Y., Li, L., Shi, X., Wang, Z., Preparation and analysis of activated carbon from sewage sludge and corn stalk. Advanced Powder Technol. 27 (2016) 684–691.

Messele, S.A., O.S.G.P. Soares, J.J.M. Órfão, F. Stüber, C. Bengoa, A. Fortuny, A. Fabregat, J.Font, Effect of activated carbon surface chemistry on the activity of ZVI/AC catalysts for Fenton like oxidation of phenol. Catalysis Today 240 (2015) 73–79.

Messele, S.A., O.S.G.P. Soares, J.J.M. Órfão, F. Stüber, C. Bengoa, A. Fortuny, A. Fabregat, J. Font, Zero-valent iron supported on nitrogen-containing activated carbon for catalytic wet peroxide oxidation of phenol. Applied Catalysis B: Environmental 154–155 (2014) 329–338.

Pereira, M.F.R., Soares, S.F., Órfão, J.J.M., Figueiredo, J.L., Adsorption of dyes on activated carbons: Influence of surface chemical groups. Carbon 41 (2003) 811–821.